ISSN 2223-3911

INDUSTRIAL TECHNOLOGY AND ENGINEERING

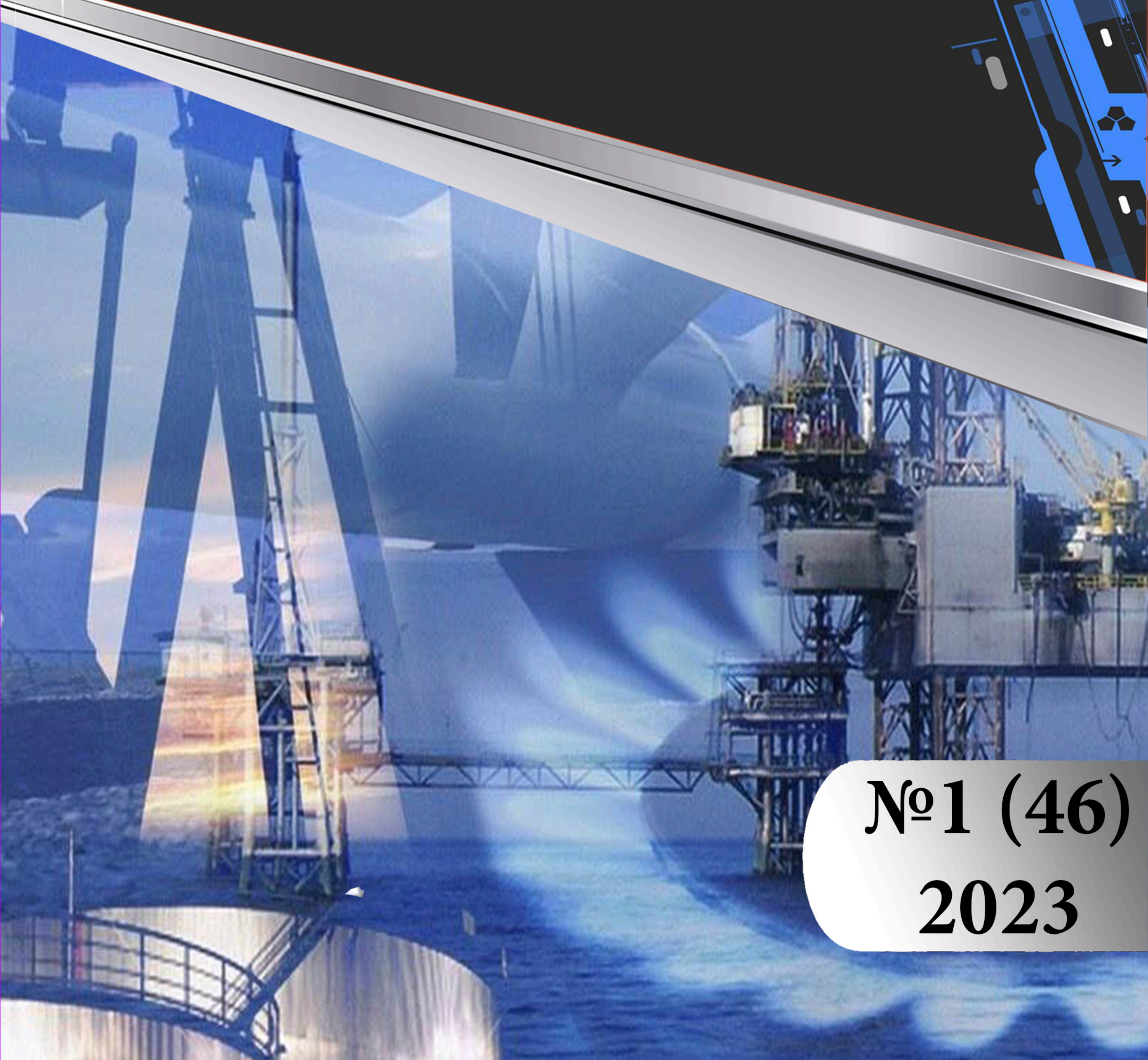

№1 (46)
2023

ISSN 2223-3911

Industrial Technology and Engineering

№ 1 (46) 2023

The journal is being published since 2011, Periodicity: 4 issues per year

Editor in chief: *D. Kozhamzharova*

The Owner: Ministry of Education and Science of the Republic of Kazakhstan
Non-Profit Joint Stock Company «M. Auezov South Kazakhstan University»

Certificate of registration of the periodic printed publication and (or) news agency № 11566-Ж issued on 04.04.2011 by Ministry of Communication and Information of the Republic of Kazakhstan.
The journal is registered at the International Centre for Registration of serial editions (UNESCO, Paris, France) in June 2011 under registration number ISSN 2223-3911.

Address:
Tauke khan avenue, 5
160012 Shymkent, Kazakhstan
Phone/Fax: +7 (7252) 21-19-82/21-19-89.
E-mail: ite_sksu@mail.ru

Printed in Kazakhstan

EDITORIAL BOARD

EDITOR –IN-CHIEF

Academician of National Academy of Sciences of the Republic of Kazakhstan, Dr.His.Sci., Professor, **Dariya Kozhamzharova**

DEPUTY OF EDITOR –IN-CHIEF

Dr.-Ing., Professor, University of Paderborn, Paderborn, Germany **Eugeny Kenig**

Dr. hab., Professor, Adam Mickiewicz University in Poznan, Poznan, Poland **Marek Sikorski**

INTERNATIONAL EDITORIAL BOARD

Mohammed Othman – PhD, Professor, University Putra Malaysia, Serdang, Malaysia.

Jamal Khatib – PhD, Professor, University of Wulverhampton, Wulverhampton, UK.

Izabella Justina Nowak – Dr.Chem.Sc., Professor, Adam Mickiewicz University in Poznan, Poznan, Poland.

Oleg Nikonov – Dr.Tech.Sc., Professor, Kharkiv National Automobile and Highway University, Kharkov, Ukraine.

Aleksandr Solovyev – Dr.Phys.-Math.Sc., Professor, M.V. Lomonosov Moscow State University, Russia.

Volodymyr Potapov – Dr.Tech.Sc., Professor, Kharkiv State University of Food Technology and Trade, Kharkiv, Ukraine.

Rufat Abiyev – Dr.Tech.Sc., Professor, Saint Petersburg State Technological Institute (Technical University), Saint Petersburg, Russia.

Josef Banas – Dr. Math.Sc., Professor, Rzeszow Polytechnic University of Technology, Rzeszow, Poland.

Oleg Poleshchuk – Dr.Chem.Sc., Professor, Tomsk State Pedagogical University, Tomsk, Russia.

Boguslawa Leska – Dr.Chem.Sc., Professor, Adam Mickiewicz University in Poznan, Poznan, Poland.

Daniele Conficoni – PhD, Professor, of the University of Padua, Padova, Italy.

Oleg Korsun – Doctor of Technical Sciences, Professor, Bauman Moscow State Technical University, Moscow, Russia.

Vyacheslav Narayev – Dr.Chem.Sc., Professor, Saint Petersburg State Institute of Technology (Technical University), Saint Petersburg, Russia.

Mohd Hasan Selamat – PhD, Associate Professor, University Putra Malaysia, Serdang, Malaysia.

Alena Meshcharakova – Cand.Econ.Sc., Associate Professor, Belarusian State Technological University, Minsk, Belarus.

Valeriy Kharchenko – Dr.Tech.Sc., Professor, All-Russian Institute for Electrification of Agriculture, Moscow, Russia.

Victoriya Yevlash – Dr.Tech.Sc., Professor, Kharkiv State University of Food Technology and Trade, Kharkiv, Ukraine.

Kazim Nadirov – Dr.Chem.Sc., Professor, M. Auezov South Kazakhstan University, Shymkent, Kazakhstan.

Murat Zhurinov – Dr.Chem.Sc., Professor, Academician of National Academy of Science of the Republic of Kazakhstan, President of National Academy of Science, Almaty, Kazakhstan.

IRSTI 61.51.81

IMPROVING THE PERFORMANCE OF REFINERIES IN THE CIS REGION – DEVELOPING AND IMPLEMENTING A PROGRAM OF EFFECTIVE RECOMMENDATIONS

Smith M.C., Ellerington T.J., Tomashevskii I.A.*, Ivashkina O.O.
HSB Solomon Associates LLC, Dallas, USA
Email: mark.smith@solomoninsight.com
***Corresponding author's email:** ivan.tomashevskii@solomoninsight.com

ABSTRACT

Improving the performance of enterprises in the energy industry of the Commonwealth of Independent States (CIS) region using the example of two refineries is described, demonstrating significant economic benefits. Both projects were completed by HSB Solomon Associates LLC (Solomon) company using their proprietary Performance Excellence Process™ (PEP™) methodology. Projects are based on the results of Solomon's benchmarking study, which is a competitive analysis of performance by comparing refineries with industry leaders. Solomon has its own proprietary benchmarking methodology for oil refining: Comparative Performance Analysis™ (CPA™) studies which mostly include the Fuels Study and the Worldwide Paraffinic Lube Refinery Performance Analysis (Lube Study) [1]. The studies evaluate the efficiency of fuels and lubes refineries. The main phases of the project implementation are described as following: Phase 1 (data diagnostics, information analysis, and interviews), Phase 2 (development and prioritization of recommendations), and Phase 3 (implementation of recommendations). The principles for selecting best practices are to evaluate current refinery operations are indicated using Solomon's library of over 4,000 best practices (with scores and comments applied across the two refineries). Each recommendation includes: description of the situation, justification for the needs of implementation, impact on refinery operations, and economic benefits. It is demonstrated that the refineries that took part in the process have created an enhanced tools to improve their operational efficiency and competitiveness. All recommendations are now getting further development and a detailed analysis. For example, refineries have taken a closer look at their DCS/APC, have conducted the pointed test runs more often, have checked the impact of implemented recommendations and monitored their key performance indicators (KPIs) after implementation of recommendations, etc.

Keywords: Performance Excellence Process (PEP), performance improvement, competitiveness and efficiency metrics, Fuels Study, consulting, key performance indicators

INTRODUCTION

For more than 20 years, enterprises of the fuels, lubes, power, and petrochemical complexes of Russia and the Commonwealth of Independent States (CIS) have been using Solomon's competitiveness and efficiency indicators to improve their operations. CIS participants' interests in Solomon's studies do not differ from those of refineries in the rest of world, which are to improve their competitiveness within increasingly competitive, globally integrated markets [1].

Today's global refining industry faces greater competitive pressure in a marketplace increasingly dominated by large new refineries that enjoy both economies of scale and the benefits of modern technology, though even size and technology alone don't guarantee success. To survive and thrive, refiners must continually work to improve performance in reliability, margin generation, and operating expense control.

Solomon's trusted benchmarking methodology and unmatched database of performance metrics show operators how they compare. With this data-driven insight, deep industry experience, and a library of best practices, we help refiners understand performance drivers, set realistic targets, and create action plans to close gaps and improve performance [2].

According to the changing future and sustainability needs, CIS enterprises' desire to improve the margin of their own refineries and different plants is growing faster, especially in the last decade (fig. 1). To do so, refineries need a powerful external force with a great knowledge of oil and gas industry and a robust methodology to make appropriate estimations.

Fig. 1. From benchmarking to performance excellence

MATERIALS AND METHODS

Solomon absolutely meets all of the requirement above and conducts benchmarking (comparative) analysis of refinery performance in all areas of refinery operation:

- Energy management
- Hydrocarbon loss
- Personnel
- Operating costs
- Carbon emissions
- Organizational effectiveness
- Planning and optimization
- Operations and technical
- Reliability and maintenance
- Quality management

With over 40 years of analysis, Solomon has gained significant data on refinery performance, with over 85% of total refining capacity regularly participating in the Worldwide Fuels Refinery Performance Analysis (Fuels Study). This refining benchmarking study is conducted biennially (in even-numbered years), and the 2020 Fuels Study was recently completed. Based on the results of the benchmarking study, a refinery will understand its current position in a wide range of metrics in relation to other refineries in the same and different regions and will be able to determine the areas of change needed to sustain or improve global competitiveness. Further, benchmarking results provide refineries with clear views of operating strengths and weaknesses relative to other refineries. In the case when the refinery understands the value of closing performance gaps, it becomes necessary to develop and implement a program to improve operations, and in this matter, the Solomon Performance Excellence Process (PEP) can help.

PEP is a process that aims to improve the work processes of a refinery in order to achieve significant economic benefits through the development and implementation of Quick-Hit and low-cost recommendations for operational improvements. Over a 2-year period in 2020 and 2021, based on the results of the Fuels Studies for 2018–2020, two refineries from the CIS expressed a desire to significantly improve their production efficiency and competitiveness. Through benchmarking it was revealed that the first refinery's energy consumption, hydrocarbon loss indicators, and product yield of process units needed improvement. Results at the second refinery revealed that the maintenance and reliability, energy consumption, hydrocarbon loss, and organizational efficiency — which affects all other indicators — are requiring improvement [3,4]. For each refinery, the total performance improvement opportunities when compared to the top five refineries in Russia and the CIS were accounted to more than 30 million United States dollars per year (M USD/yr).

Solomon met with the refineries' top management and proposed implementing formal PEP projects, with each project including three main phases as detailed below.

RESULTS AND DISCUSSION

Phase 1 – Data Diagnostics, Information Analysis, and Interviewing (Best Practices Assessment)

In Phase 1, a group of Solomon subject matter experts (SMEs) evaluated refinery operations using a range of methods and approaches to achieve a clear understanding of current refinery operating practices including detailed data diagnostics.

The Best Practices Assessment (BPA) and overall evaluation has two goals: 1) gaining an understanding of the root causes of the performance gaps identified in the Solomon Fuels Study, and 2) comparing refinery work process flows and practices with those of the industry leaders.

In addition, Solomon used its Energy Diagnostic Tool to evaluate energy efficiency and create recommendations for energy intensity improvements. A detailed energy analysis was used to determine the causes of numerous energy-related gaps and identify where to focus improvement efforts. Solomon conducted Energy Analysis using the data resulting from the refiner's participation in Solomon's Fuels Study. This data was then supplemented with current operational data that allowed Solomon to perform diagnostic analysis of key energy consumption parameters (e.g., amine systems operating variables, temperatures of feeds to units, stripping steam usage, etc.). The evaluation was performed according to the Solomon energy efficiency metrics. The same tool is also used for other sites in terms to evaluate the performance and make it better [5].

As a result of Phase 1, each refinery received hundreds of Best Practice Scorecards. The scores and comments were provided and verified by personnel from each refinery. In addition, based on the results of work at this phase, "Quick-Hit" improvement recommendations were identified. These are recommendations that bring a very quick (within 2–3 months) economic benefit.

Phase 2 – Development and Prioritization of Recommendations

Solomon developed detailed recommendations for improving the client's established work practices that were below the best practice performance threshold to move the client's performance to the best practice level.

Based on the analysis and work in Phase 1, one refinery received 35 recommendations (including 6 "Quick-Hit"), and a second - 46 recommendations (including 11 "Quick-Hit") to improve their operational efficiency. The description of each recommendation included an evaluation of current working practices, the purpose of the recommendation of the processes and/or practices for which the recommendation was made, the justification, and the impact of implementation. Most of the recommendations delivered measurable value. Other "enabler" recommendations supported existing work process changes to move to excellent and good practices and allowed other opportunities to deliver measurable value. Before reporting on the detailed recommendations, all were reviewed and agreed upon by the client's team members involved in the PEP work. As a result of the projects conducted at the two refineries, 81 total recommendations were developed with a total economic benefit of 70M USD/yr. Since a large number of detailed recommendations were issued at the same time, those of highest priority were scheduled to be implemented first, with the others to follow.

Phase 3 – Implementation of the Recommendations

Finally, Phase 3 includes implementation of opportunities.

For implementation, Change Management Teams (CMTs) were created to review implementation progress, manage project resources, monitor the pace of implementation of Quick-Hits and detailed recommendations, and resolve resource constraints.

Then, Best Practice Teams (BPTs) or implementation teams were created for each improvement area. The teams consisted of 5–8 refinery SMEs (who were served as cross-functional representatives) with the knowledge, experience, and skills required in maintenance and reliability, energy, and hydrocarbon losses. The individuals were responsible for providing input and ideas on the implementation of the PEP recommendations, actively participating in developing specific implementation action plans for each recommended change, providing active guidance for the implementation of new draft PEP recommendations and related working practices, discussing barriers to progress, and offering options for removing obstacles. From Solomon's experience, the implementation of each recommendation goes through four main psychological phases (refer to Fig. 2). Solomon supports the client teams as they navigate through these personal and organizational stages.

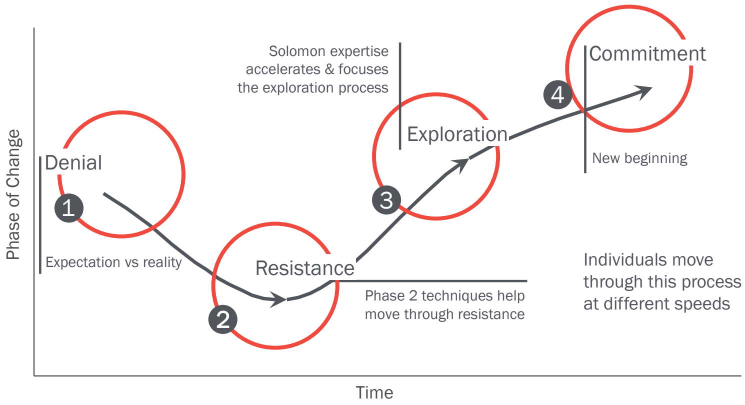

Fig. 2. The Process of Implementing the Recommendations

Implementation plan progress for each recommendation is regularly reviewed by the BPTs until the recommended implementation actions are completed and the recommendation is firmly in place with benefits validated. Next, the implementation impact on production performance is monitored over the next 12 months. For the two refineries mentioned above, selected recommendations at each refinery (about 15% of the total number) were implemented even before the completion of the PEP project. At the end of each PEP project, client participants were recognized with letters of appreciation for their commitment and efforts.

If summarize, Performance Excellence Process has the following deliverables:

- Conduct data diagnostics to identify opportunities and focus the best practice assessment.
- Evaluate existing behaviors, work processes, procedures, and practices that drive a site’s performance and operation.
- Use results to accelerate the change process and create a framework for continuous improvement.
- Initial results in 8–10 weeks, with typical benefit reaching 20–40% gap closure.
- Blend technical and behavior changes needed to create sustainable results.
- Support continuous improvement with health checks and special topic workshops.

CONCLUSION

. Operating in an increasingly complex business environment of economic cycles and regulatory changes is often difficult to navigate. High-cost, short-term solutions such as cutting costs, reducing headcount, and making major capital investments may not generate sustainable, long-term success.

Solomon’s PEP is a proven, efficient, and reliable approach for improving refinery performance, from the level of individual units to the entire refinery and organization as a whole [6]. This PEP methodology is based on Solomon’s unmatched industry data that, when combined with the expertise of Solomon’s SMEs in each focus area of opportunity, enables confident and low-risk improvement across the most impactful areas of refinery operation, including energy efficiency, maintenance, reliability, plant yields, and hydrocarbon losses

This process leverages unique data, proven processes, and expert guidance, to deliver insight and recommendations you can trust. Solomon evaluate important drivers of your operational performance and identify “quick-hit” improvement opportunities and collaborate with you to improve business processes and work practices to sustain improvement [7].

Due to the successful implementation of the projects highlighted above, other refineries from the CIS countries have expressed interest in pursuing similar PEP improvement actions at their own refineries.

REFERENCES

1. Brown R.F., Shishorin Yu.R., Ivashkina O.O., Kapustin A.V. Benchmarking of Russian refineries: 15 years in Russia. Automation in industry, 2015, no. 4, pp. 46-53.
2. https://www.solomoninsight.com/industries/refining/
3. Shishorin Yu.R., Rybkin V.I., Ellerington T., Power P. Improving operational efficiency and benchmarking Russian energy companies. Reports at the 11th Honeywell Russian Technology Conference. Moscow, 2018.
4. Ellerington T., Power P., Shishorin Yu.R., Aksenova T.S. Increasing operating efficiency and benchmarking of russian enterprises in the energy sector (by the example of refinery). Automation in industry, 2018, no. 12, pp. 34-41.
5. South American Refiner Sets Ambitious Goal to Improve Energy Efficiency, Lower Costs, and Reduce Carbon Emissions. Available at: https://www.solomoninsight.com/assets/files/South-American-Refiner-Sets-Ambitious-Goal-Improve-Energy-Efficiency-Lower-Costs-and-Reduce-Carbon-Emissions.pdf
6. PEP process (2017). Available at: https://www.solomoninsight.com/blog/performance-excellence-process-closing-the-gap. (accessed Jun 21, 2017)
7. Performance improvement…accelerated. Close gaps. Achieve results. Trusted insight and recommendations (2023). Available at: https://www.solomoninsight.com/services/advisory-services/performance-excellence

IRSTI 661.9:532.259

Ismailov B.R., Suleimen O.M.[*]
M. Auezov South Kazakhstan University, Shymkent, Kazakhstan
[*]***Corresponding author's e-mail:*** *olzhas.suleimen@auezov.edu.kz*

MODELING OF A VISCOUS FLUID FLOW AROUND A RECTANGULAR OBJECT IN TECHNOLOGICAL DEVICES

ABSTRACT

This article presents the results of modeling the flow of a viscous fluid and its interaction with solids (rectangular objects). Such processes take place in technological devices that allow liquid to flow around various nozzles. This article describes the algorithm and the results of the software implementation to solve the problem. The program is based on solving the Navier-Stokes equations in two-dimensional Cartesian coordinates by the finite difference method. The computation uses a fully staggered grid to store velocity components and pressure. The advantage of this grid is that the pressure is placed in the center of the cell and the velocity separately at the edge of the cell. This helps avoid many stability problems in the pressure Poisson equation. We chose the Python programming language to write the program and visualize the results. By providing the necessary conditions, we can use the program to develop physical and mathematical models of processes occurring in heat and mass transfer devices.

Keywords: Navier-Stokes, heat and mass transfer, staggered grid, numerical method, python, velocity

INTRODUCTION

Various industries utilize a range of technological devices including heat and mass transfer apparatuses such as columnar multichannel mass transfer apparatuses. These apparatuses, including absorbers, scrubbers and contact devices (packed, cascade, bubbling), facilitate the interaction of liquid and gas flows. Despite their varying purposes, these devices operate according to similar laws.

The Navier-Stokes equations are used in this article because they model two important physical laws: momentum conservation and continuity. These equations, in turn, allow us to simulate the flow of a viscous fluid and its interaction with a solid body in mass transfer apparatus channels. We can generalize theoretical information about the processes that occur in apparatuses by using a mathematical model with correctly specified boundary conditions. This enables us to conduct systematic numerical experiments to calculate the main dynamic characteristics of the process under investigation, including problems of optimizing the regime and geometric characteristics of the apparatus.

We can write user programs and algorithms in one of the algorithmic languages to solve numerically and simulate the flow around a rectangular object in a mass transfer device. The Navier-Stokes equations are increasingly being modelled and numerically solved by researchers using software programs in recent years. We selected Python for this task because of its tremendous potential benefits in the areas of computational mathematics.

Python is an interpreted, high-level, object-oriented, general-purpose dynamic programming language. In the field of scientific computing, Python has the following important advantages over MATLAB:

- Code quality;
- Portability;
- Flexibility;
- Productivity;
- Availability of packages;
- Cost [1].

MATERIALS AND METHODS

Theoretical analysis. The Navier-Stokes equations are differential equations that account for the viscosity of a fluid or gas when describing the motion of a continuous medium. A simple model of molecular interactions was used by L. Navier to make this deduction in 1822. These equations were developed in a modern version by J. Stokes in 1845 as a consequence of his research on the stationary motion of an incompressible fluid utilizing the principles of momentum and mass conservation for a continuous medium.

In the simplest case of motion of an incompressible (density ρ is constant) and non-heat-conducting (temperature T is constant) medium, the Navier-Stokes equations in vector form have the form:

$$\frac{\partial \vec{V}}{\partial t} + \vec{V} \cdot \nabla \vec{V} = -\frac{1}{\rho} \nabla p + \eta \Delta \vec{V} + \vec{F} \tag{1}$$

where $\vec{V}$ – is the fluid particle velocity, t – is time, $\vec{F}$ – is the external specific (per unit mass) force, p – is the pressure, $\eta = \mu / \rho$ – is the kinematic viscosity coefficient (μ – is the dynamic viscosity coefficient), ∇ – is the Nabla operator, Δ – is the Laplace operator. Viscosity coefficients depend on temperature and, as a rule, are determined experimentally for a liquid, and derived from the kinetic theory of gases for a gas [2].

The representation of equation (1) in a two-dimensional Cartesian coordinate system has the following form:

$$\begin{cases} \dfrac{\partial u}{\partial t} + u\dfrac{\partial u}{\partial x} + \vartheta\dfrac{\partial u}{\partial y} = -\dfrac{1}{\rho}\dfrac{\partial p}{dx} + \eta\left(\dfrac{\partial^2 u}{\partial x^2} + \dfrac{\partial^2 u}{\partial y^2}\right) \\ \dfrac{\partial \vartheta}{\partial t} + u\dfrac{\partial \vartheta}{\partial x} + \vartheta\dfrac{\partial \vartheta}{\partial y} = -\dfrac{1}{\rho}\dfrac{\partial p}{dy} + \eta\left(\dfrac{\partial^2 \vartheta}{\partial x^2} + \dfrac{\partial^2 \vartheta}{\partial y^2}\right) \\ \dfrac{\partial u}{\partial x} + \dfrac{\partial \vartheta}{\partial y} = 0 \end{cases} \tag{2}$$

An approach for numerical solution of system (2) in Helmholtz variables is provided by [3], which mimics the gas flow around regularly positioned plate nozzles in the contact device of column mass transfer devices (current function–vorticity). It was implemented using a

Turbo Pascal application. It is necessary to create a software for creating current isolines, which is a separate task, in order to process numerical data in the form of a matrix of velocity values while taking into consideration the multichannel interaction of the gas flow with the wall and nozzles.

The numerical solution of the Navier-Stokes equations using the right-handed difference approximations and the markers and cells approach, is presented in [4]. The resultant solution may be used to represent a fluid with a free surface since it is created in the form of basic physical variables and is not reduced to a solution in the form of vortex variables and a current function. When modeling aquatic bodies, this is employed (lakes, rivers, reservoirs, and others). Nonlinear terms are used to express the differential equations that have been solved and describe fluid motion. Because of this, finding a solution takes more work, but the formulae we get allow us to accurately describe how the simulated fluid circulates. Based on the formulas obtained, it is possible to develop hydrodynamic models of reservoirs and use them to simulate the transfer of heat and impurities

Numerical method. The problem is solved numerically using the finite difference method.

The finite difference method is a numerical method for solving differential equations using a difference scheme instead of derivatives. This is one of the grid methods.

To solve an elliptic problem using the finite difference method, create a mesh in the computational domain, then choose a difference scheme, and write a difference equation (similar to the original equation, but using the difference scheme) for each mesh node, and then consider the boundary conditions. If we take the system of linear algebraic equations and solve it, we will get an approximation of the nodal solution.

A great advantage of this approach is that the problem is less dependent on the boundary conditions, the geometry of the structure and the nature of the initial stress state. The disadvantage is the high order of the algebraic equation system. Another feature of the finite difference method is the consideration of the complexity of mixed boundary conditions, which are described by different differential equations, where multi-connected domains and conjugates of domains are considered.

The main problem of the method is the creation of a correct difference scheme approaching the solution. The construction of the circuit is based on the properties of the initial differential operator [5].

There are different possibilities to discretize PDEs such as the Navier-Stokes equation or the Poisson equation on grids. In the 2d case of the Navier-Stokes equations, we have three unknowns on the grid: pressure p, x-direction velocity u, y-direction velocity ϑ.

The easiest way is to put all the information at one point on the grid. Such grids are called collocated grids. A small outcut of a collocated grid is depicted in Fig. 1 (a).

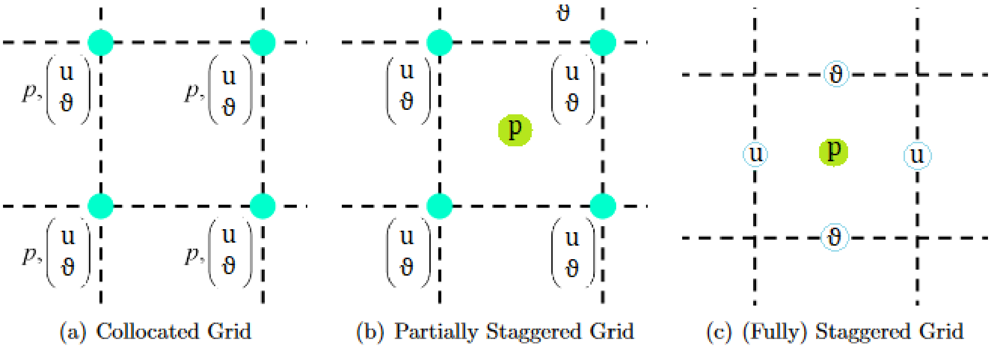

Fig. 1 - Grid types depending on the data locality

A separation of the pressure and velocities but storing the velocities at one point leads us to a so-called partially staggered grid (Fig. 1 (b)). A fully staggered grid is a grid, where the pressure is placed in the cell center and the velocities are placed separately on the edges of the cell. A sketch of a fully staggered grid can be seen in Fig. 1 (c). Collocated grids lead to a number of stability problems for our pressure Poisson equation. We thus concentrate on the case where the unknown (pressure) is placed at the center of the cell [6]. For our problem, we use a fully staggered grid, which is shown in Fig. 2.

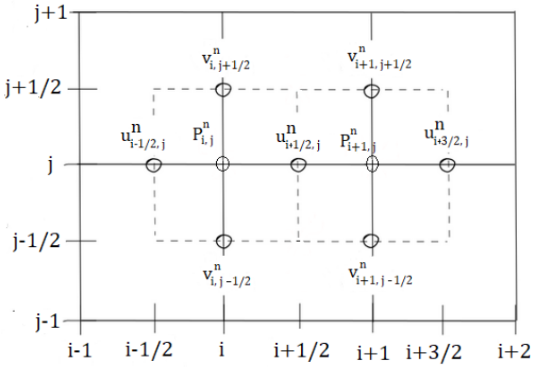

Fig. 2 – Staggered grid

Discretization of equations for velocity components u and ϑ and the pressure p. The discrete momentum equations u and ϑ at internal nodes are given by

$$a_P^{int} u_{i-1,j} + a_N^{int} u_{i-1,j+2} + a_S^{int} u_{i-1,j-2} + a_W^{int} u_{i-3,j} + a_E^{int} u_{i+1,j} = \frac{\hat{P}_{i-2,j} - \hat{P}_{i,j}}{2\rho\Delta x}$$

$$b_P^{int} u_{i,j+1} + b_N^{int} u_{i,j+3} + b_S^{int} u_{i,j-1} + b_W^{int} u_{i-2,j+1} + b_E^{int} u_{i+2,j+1} = \frac{\hat{P}_{i,j} - \hat{P}_{i,j+2}}{2\rho\Delta y}$$

where

$$a_P^{int} = \frac{\hat{u}_{i-1,j}}{2\Delta x} + v\left(\frac{1}{2\Delta x^2} + \frac{1}{2\Delta y^2}\right)$$

$$a_N^{int} = \frac{\hat{u}_{i-1,j}}{4\Delta y} - \frac{v}{4\Delta y^2}$$

$$a_S^{int} = -\frac{\hat{u}_{i-1,j}}{4\Delta y} - \frac{v}{4\Delta y^2}$$

$$a_W^{int} = -\frac{\hat{u}_{i-1,j}}{2\Delta x} - \frac{v}{4\Delta x^2}$$

$$a_E^{int} = -\frac{v}{4\Delta x^2}$$

$$b_P^{int} = \frac{\hat{u}_{i,j+1}}{2\Delta x} + v\left(\frac{1}{2\Delta x^2} + \frac{1}{2\Delta y^2}\right)$$

$$b_N^{int} = \frac{\hat{u}_{i,j+1}}{4\Delta y} - \frac{v}{4\Delta y^2}$$

$$b_S^{int} = -\frac{\hat{u}_{i,j+1}}{4\Delta y} - \frac{v}{4\Delta y^2}$$

$$b_W^{int} = -\frac{\hat{u}_{i,j+1}}{2\Delta x} - \frac{v}{4\Delta x^2}$$

$$b_E^{int} = -\frac{v}{4\Delta x^2}$$

Variables with a caret above them are quantities that were calculated in the previous iteration. Due to the use of a collocated grid, the values of ϑ in the u-momentum equation and u in the ϑ-momentum equation appearing as coefficients of the convective derivatives are not available at the desired points.

These velocities are therefore computed to second order accuracy using the velocities of the four surrounding grid nodes in which they are stored.

$$u\,|_{i,j+1} = \frac{u_{i+1,j} + u_{i+1,j+2} + u_{i-1,j} + u_{i-1,j+2}}{4}$$

$$\vartheta\,|_{i,j+1} = \frac{\vartheta_{i,j-1} + \vartheta_{i,j+1} + \vartheta_{i-2,j-1} + \vartheta_{i-2,j+1}}{4}$$

The discrete equations of the u -momentum at the boundary nodes are the same as at the internal nodes, with some modifications.

For example, the discrete equations of the u -momentum at the input nodes are the same as those at the internal nodes, except that the value of $u_{1,j}$ is known [7].

Pressure correction equations for lower nodes:

$$c_P^{int}\, p'_{i,j} + c_E^{int}\, p'_{i+2,j} + c_W^{int}\, p'_{i-2,j} + c_N^{int}\, p'_{i,j+2} + c_S^{int}\, p'_{i,j-2} = \frac{u^*_{i-1,j} - u^*_{i+1,j}}{2\Delta x} - \frac{\vartheta^*_{i,j+1} - \vartheta^*_{i,j-1}}{2\Delta x}$$

where

$$c_P^{int} = \frac{1}{4\rho\Delta x^2 a_{i+1,j}} + \frac{1}{4\rho\Delta x^2 a_{i-1,j}} + \frac{1}{4\rho\Delta y^2 b_{i,j+1}} + \frac{1}{4\rho\Delta y^2 b_{i,j-1}}$$

$$c_E^{int} = -\frac{1}{4\rho\Delta x^2 a_{i+1,j}}$$

$$c_W^{int} = -\frac{1}{4\rho\Delta x^2 a_{i-1,j}}$$

$$c_N^{int} = -\frac{1}{4\rho\Delta y^2 b_{i,j+1}}$$

$$c_S^{int} = -\frac{1}{4\rho\Delta y^2 b_{i,j-1}}$$

Solution algorithm. The program algorithm for solving the problem of a viscous fluid flow around a rectangular object is as follows:

1. Initialization:

a) Initialize the speed u

b) Initialize the speed ϑ

c) Initialize pressure p (uniformly zeros)

2. Upgrade the speeds u (+Boundary conditions)

$$u \leftarrow u + dt \cdot \left(-\frac{\partial p}{\partial x} + \nu\,\nabla^2 u - \frac{\partial u^2}{\partial x} - \vartheta\,\frac{\partial u}{\partial y} \right)$$

3. Upgrade speeds ϑ (+Boundary conditions)

$$\vartheta \leftarrow \vartheta + dt \cdot \left(-\frac{\partial p}{\partial y} + \nu \nabla^2 \vartheta - u \frac{\partial \vartheta}{\partial x} - \frac{\partial \vartheta^2}{\partial y} \right)$$

4. Calculate the Divergence of the Prevelocity Components

$$d = \frac{\partial u}{\partial x} + \frac{\partial v}{\partial y}$$

4. Solve the Poisson problem to correct the pressure q

$$\text{solve } \nabla^2 q = \frac{d}{dt} \text{ for } q$$

5. Upgrade the pressure

$$p \leftarrow p + q$$

6. Upgrade speeds to be incompressible

$$u \leftarrow u - dt \cdot \partial q / \partial x$$

$$v \leftarrow v - dt \cdot \partial q / \partial y$$

7. Now, we need to repeat cycle until we reach steady state.

RESULTS AND DISCUSSION

Using a computer program written in Python, we obtained the following results (Fig. 3-6):

To simulate a viscous liquid, the program used a low value of Reynolds number.

In Fig. 3 you can observe the region where the vortices form. In other words, when a fluid flows around a rectangular body, we can consider the four main regions to be vortex regions.

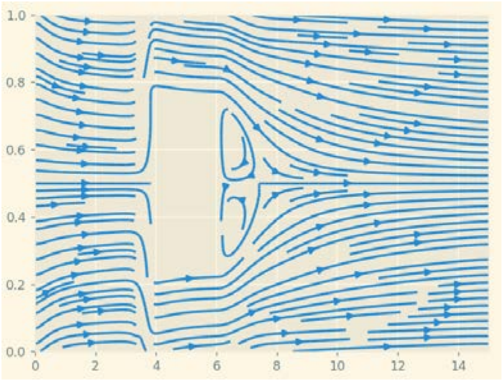

Fig. 3 - Visualization of the flow of a viscous fluid around a rectangular object

Fig. 4 shows the initial state of the thread. As we can see, after the collision of the flow with a rectangular object, it moves to the limit of the channel, and vortices are formed there.

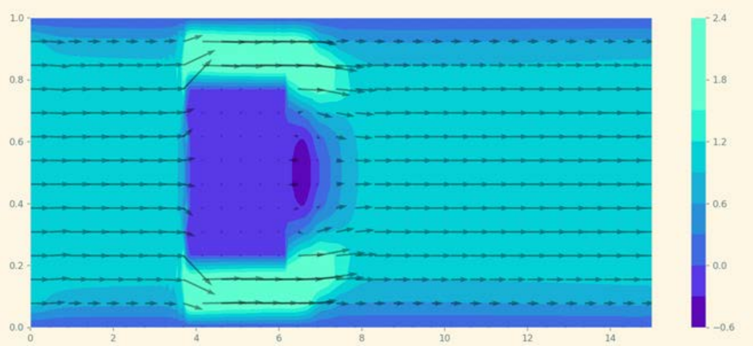

Fig. 4 - Start of rendering

Fig. 5 shows the end of the rendering. As we can see, the Hagen-Poiseuille profile is fully developed, and the vortex regions after the object are fully formed.

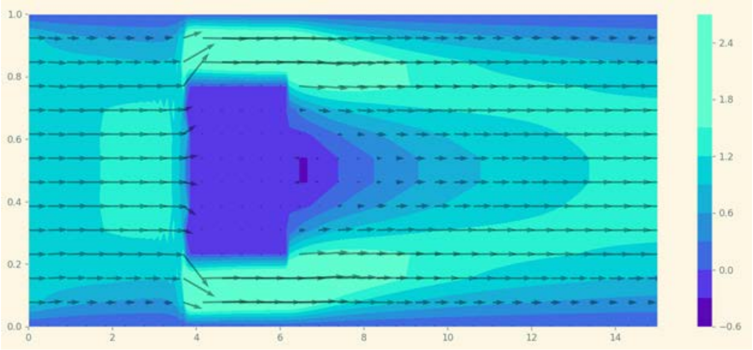

Fig. 5 - End of rendering

Fig. 3-5 show that when a viscous fluid flows around a rectangular object, it develops vortex zones where vortices are created due to flow separation.

During the simulation, the flow produces a Hagen-Poiseuille profile. After this stage, the flow becomes regular over the entire cross-section and forms a parabolic profile with a larger diameter. By the end of the zone, the flow is fully developed and meets the outflow boundary condition. An implementation of the high Reynolds number model is shown in Fig. 6.

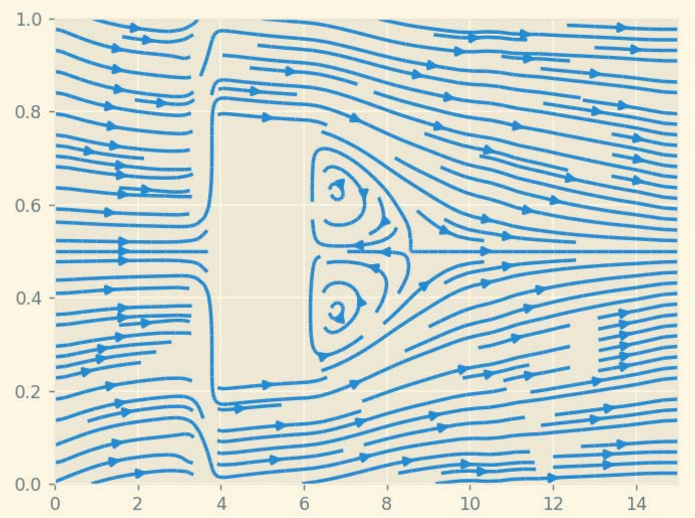

Fig. 6 – Simulation at high values of the Reynolds numbers

CONCLUSION

A program algorithm was developed to solve the problem of viscous fluid flow around rectangular objects. The program is compiled according to an algorithm. By providing the necessary initial conditions, it can be used to develop physical and mathematical models of processes occurring in heat and mass transfer devices.

The presented method of visualizing the numerical results of the solution of the Navier-Stokes equations allows for a systematic numerical experiment to determine the locations and sizes of the vortex and stagnant zones in the contact zones of chemical optimization technology devices.

REFERENCES

1 Jia Liu, Lina Wu, Xingang Fang. Using Python to Solve the Navier-Stokes Equations - Applications in the Preconditioned Iterative Methods. *Journal of Scientific Research & Reports*, 2015, vol. 7, is. 3, pp. 207-217, DOI: https://doi.org/10.9734/JSRR/2015/17346

2 Sylvio R. Bistafa. On the development of the Navier-Stokes equation by Navier. *Revista Brasileira de Ensino de F ́ısica*, 2017, vol. 40, no. 2, DOI: https://doi.org/10.1590/1806-9126-RBEF-2017-0239

3 Bakhtiyar Ismailov, Leyla Musabekova, Zhanat Umarova, Khairulla Ismailov, Kuttybek Arystanbayev. Mathematical and computer simulation of particle redistribution and inertial swarming in dispersed systems. *Indonesian Journal of Electrical Engineering and Computer Science*, 2022, vol. 28, no. 2, pp. 909-917, DOI: https://doi.org/10.11591/ijeecs.v28.i2.pp909-917

4 Baklagin B. N. Primer chislennogo resheniya uravneniy Nav'ye-Stoksa metodom markerov i yacheyek dlya modelirovaniya vodnykh ob"yektov [An example of numerical solution of the Navier-Stokes equations by the method of markers and cells for modeling water bodies]. *Sovremennye problemy nauki i obrazovaniia*, 2014, no. 5. Available at: https://science-education.ru/ru/article/view?id=15264

5 Litvinova, E.V. Primeneniye metoda konechnykh raznostey dlya resheniya dinamicheskikh zadach [Application of finite differences method for dynamic problems

solution]. *International Research Journal*, 2017, no. 6(60), part 3, DOI: http://doi.org/10.23670/IRJ.2017.60.094

6 Michael L. A Full Multigrid Implementation on Staggered Adaptive Cartesian Grids for the Pressure Poisson Equation in Computational Fluid Dynamics. Master’s thesis. München, Technische Universität München, 2008, 76 p.

7 Nursalasawati Rusli, Erwan Hafizi Kasiman, Kueh Beng Hong Ahmad, Airil Yasreen Mohd Yassin, Norsarahaida Amin. Numerical Computation of a Two-Dimensional Navier-Stokes Equation Using an Improved Finite Difference Method. *MATEMATIKA: Malaysian Journal of Industrial and Applied Mathematics*, 2011, vol. 27, pp. 1–9.

IRSTI 661.9:532.259

ABOUT THE NUMERICAL SOLUTION OF THE HEAT EQUATION AND STABILITY CONDITIONS

Ismailov B.R., Rakhmetullakyzy A.*
M. Auezov South Kazakhstan University, Shymkent, Kazakhstan
***Corresponding author's e-mail:** aisulu.rakhmetullaqyzy01@auezov.edu.kz*

ABSTRACT

The issue of temperature dispersion in a consistent center with primary conditions at the boundary is being examined. A numerical solution was obtained having utilized a finite differential method along with an implicit method for the derivative approximation scheme. We will explore boundary problems, utilizing finite differential methods, that simulate heat transmission. These problems will simulate heat radiation over a plain infinite plate or an insulated rod. The flat infinite plate or insulated rod will have one boundary with a constant temperature of T_l and the other boundary with temperature T_n. The plate will have an initial temperature T_0, with no internal heat sources.

Real physical processes take place in time and space, which has three dimensions. When constructing difference schemes, the transition to multidimensional problems of thermal conductivity does not cause fundamental difficulties. However, the number of unknowns in the system of difference equations increases significantly, the number of arithmetic operations necessary to solve it increases.

Keywords: Numerical modeling of heat exchange processes, the finite difference method, analytical methods, approximating.

INTRODUCTION

The importance of numerical modeling in predicting heat transfer processes is on the rise as modern science and technology require reliable forecasts of such processes, and experimental research under laboratory or field conditions can be difficult, costly, or unfeasible. The successful application of numerical modeling in research, design, and production institutions is increasing. In applied problems, there is often a need to deal with the issue of temperature distribution under various boundary and initial conditions. Mathematically, this problem serves as a testing ground for creating various theories regarding the existence and uniqueness of solutions. While there are analytical methods available for solving the problem of thermal conductivity, the solutions are usually in the form of a functional series, and approximation techniques are often necessary for their computation [1].

MATERIALS AND METHODS

One of the effective techniques for resolving applied issues is currently the finite difference method. In accordance with the semantics and precision requirements of the issue, explicit and implicit plans are utilized. Efficient numerical schemes have been created in the literature on numerical methods to solve heat transfer problems for three types of initial-boundary problems. Yet, in order to use in applied problems (e.g., physics), it is essential to precisely define problems with experiments utilizing various schemes and understand numerical results [2].

The capacity of transferring heat energy from one point to another between body points with a temperature difference is thermal conductivity. The potential and kinetic energy of molecules increase as a body heats up, causing the particles in a solid to oscillate more vigorously while maintaining their equilibrium state. From one particle to another, excess energy is transferred, namely from one portion of the body to others. Different types of power are given by all solids.

We consider boundary problems simulating heat transfer through a flat infinite plate or an insulated rod in Fig.1. on the same border plates supported stable temperature T_l, and the temperature on the other boundary T_n. Initial temperature T_0, There are no sources of heat inside the plate.

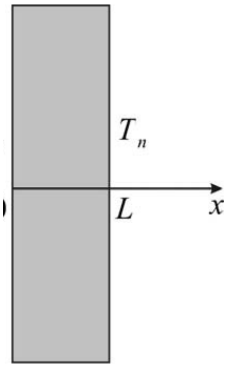

Fig. 1. Geometry of the heat transfer calculation

In these circumstances, the temperature shifts solely in the perpendicular direction of the plate boundary. If we take look at Fig. 1, and position the x-axis in a horizontal manner, the temperature in the O_x and $O_z$directions labeled as constant. In addition, we consider a constant thermophysical characteristic even with temperature alterations. As a result, equation (1) of the differential thermal conductivity equation transcends into the subsequent form:

$$\rho c\frac{\partial T}{\partial t}=\lambda\frac{\partial^2 T}{\partial x^2},0<x<L \tag{1}$$

$$\begin{aligned} &t=0:T=T_0,0\le x\le L\\ &x=0:T=T_l,t>0\\ &x=L:T=T_n,t>0 \end{aligned} \tag{2}$$

In order to give a complete mathematical description of the considered problem, (2) it is necessary to set the physical conditions of uniqueness. If the plate is made of steel, then $\lambda\lambda=46W/(m\cdot°C)$, $\rho=7800kg/m^3$, $s=460J/(kg\cdot°C)$ [3].

The finite difference method is employed to solve the mathematical formulation of this issue, utilizing a uniform grid. The plate is divided into N-1 identical intervals, depicted in Fig. 2 as the finite difference grid.

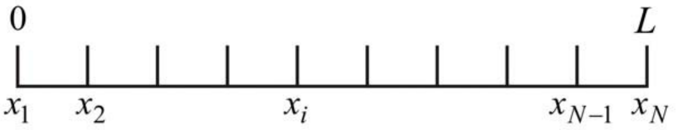

Fig. 2. Finite difference mesh:
$x_2, x_3, \ldots, x_{N-1}$ coordinates of internal nodes;
x_1, x_N coordinates of boundary nodes.

The temperature value at the i-th node at time t = as $t_n = n \cdot \tau$., where the step represents integration across time coordinates and n denotes the time step. The differential operators in (3) are substituted with their corresponding finite-difference equivalents using an implicit scheme.

$$\begin{gathered} \frac{dT}{dt} = \frac{dT_i^{n+1} - T_i^n}{\tau}, \\ \frac{\partial^2 T}{\partial x^2} = \frac{T_{i+1}^{n+1} - 2T_i^{n+1} + T_{i-1}^{n+1}}{h^2} \end{gathered} \tag{3}$$

As a result of approximating individual derivatives through finite differences, a system of linear algebraic equations is obtained.

$$\rho c \frac{T_i^{n+1} - T_i^n}{\tau} = \lambda\left(\frac{T_{i+1}^{n+1} - 2T_i^{n+1} + T_{i-1}^{n+1}}{h^2}\right), i = 2, \ldots., N-1, \geq 0 \tag{4}$$

Scheme for approximating partial derivatives can be represented graphically as follows in Fig.3.

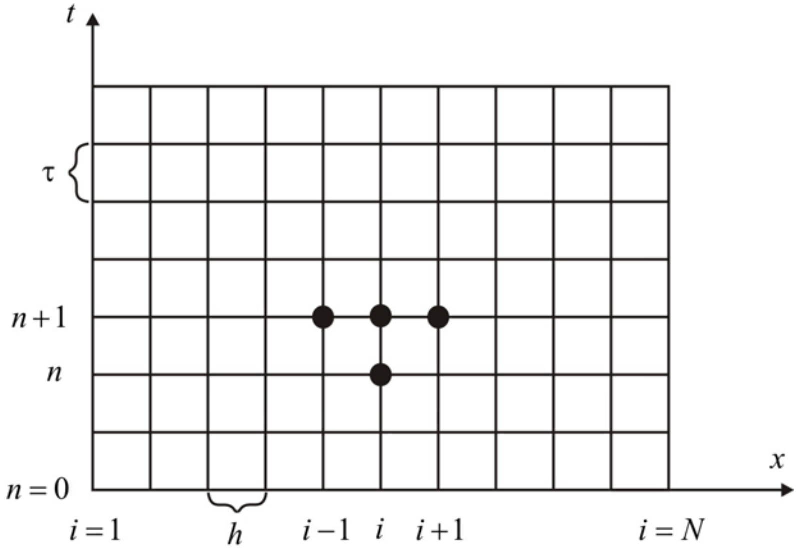

Fig. 3. Hidden four-point difference scheme view

It is evident from Fig. 3 that a scheme utilizing a difference of four points is employed, with three points originating from the fresh time layer and one from the previous one [4].

The approach to count approximations for the derivatives that has been outlined is referred to as implicit, as the temperature field in the modern time layer is articulated implicitly, meaning that solving the set of equations (5) is a requisite to obtain it.

The resulting set can be simplified to attain the most common structure:

$$\begin{aligned} &A_i T_{i+1}^{n+1} - B_i T_i^{n+1} + C_i T_{i-1}^{n+1} = F_i \\ &A_i = C_i = \frac{\lambda}{h^2}, B_i = \frac{2\lambda}{h^2} + \frac{\rho c}{\tau}, \\ &F_i = -\frac{\rho c}{\tau} T_i^n \end{aligned} \tag{5}$$

System (6) has a three-diagonal structure. Since a non-stationary problem is determined, system (6) must be solved at each time step. Suppose there is such a set of numbers $\alpha_i, \beta_i (i = 1, N-1)$ for that, the second-order three-point equation (6) is transformed two-point first-order equation. (7) :

$$\begin{aligned} &A_i T_{i+1}^{n+1} - B_i T_i^{n+1} + C_i T_{i-1}^{n+1} \alpha_{i-1} + C_i \beta_{i-1} = F_i \\ &T_i^{n+1} = \frac{A_i}{B_i - C_i \alpha_{i-1}} T_{i+1}^{n+1} + \frac{C_i \beta_{i-1} - F_i}{\beta_i - C_i \alpha_{i-1}} \end{aligned} \tag{6}$$

If i =2,3,…, it exactly matches with it. N -1

$$\alpha_i = \frac{A_i}{B_i - C_i \alpha_{i-1}}, \beta_{1=} \frac{C_i \beta_{i-1} - F_i}{\beta_i - C_i \alpha_{i-1}} \tag{7}$$

To determine α_i, β_i the necessity, knowledge of the left boundary condition (3) is required. Furthermore, application of formulas (9) will T_2^{n+1} yield a solution only if the $T_{N+1}^{n+1}, T_{N+2}^{n+1}$ appropriate right boundary condition (4) is also found. The solution process for equations of type (8) using this method involves three formulas: α_i, β_i computation of the sweeper coefficients according to formulas (12), followed by use of the said coefficients $T_N^{n+1} \cdot h, i = N-1, N-2.....2$ to calculate the unknowns using formula (8), provided that the delimiters remain constant and are not removed. The correctness of the sweep is ensured when $|a_i| < 1$ all I = 1, N-1. The aforementioned theorem provides adequate conditions for the proper arrangement and stability of the equation [5].

$$\forall_i = 2, N-1, |\alpha_i| < 1 \tag{8}$$

Performed automatically in many applications of the method. We determine the sweep coefficients and recreate the complete algorithm for solving the obtained system. Bx =0 T =T$_l$ after that

$$\begin{aligned} &T_i^{n+1} = \alpha_1 T_2^{n+1} + \beta_1 = T_l \\ &\alpha_1 = 0, \beta_1 = T_l \\ &x = LT = T_n \\ &T_N^{n+1} = T_n \end{aligned} \tag{9}$$

Differential relations approximating the differential problem (1)-(4) have shown:

$$\begin{aligned} &\rho c \frac{T_i^{n+1} - T_i^n}{\tau} = \lambda \cdot (\frac{T_{i+1}^{n+1} - 2T_i^{n+1} + T_{i-1}^{n+1}}{h^2}), i = 2..., N - 1 n \geq 0 \\ &T_1^0 = T_0, i = 2..., N - 1; T_1^n = T_l, n > 0 \\ &T_N^n = T_n, n > 0 \end{aligned} \tag{10}$$

The approximation of the differential problem (1)-(4) to the finite-difference problem (14)-(17) is performed with first-order accuracy in time t and second-order in the spatial coordinate h. In this case, the implicit difference scheme is absolutely stable, i.e. it is possible to implement the integration of the boundary value problem with any difference time step. The time step is chosen so that the entire time interval is divided into at least 10 steps [6].

RESULTS AND DISCUSSION

Calculation results according to the above program after 60 seconds of the heating process is shown in Fig. 4.

$$L = 0.1m; \frac{\rho}{u} \cdot 0.03d = 7800 \frac{kg}{m^3}; \frac{s}{u} \cdot 0.03d = 460 \frac{J}{kg \cdot {}^\circ C}; T_0 = 20^\circ C; T_l = 300F; T_n = 100^\circ C$$

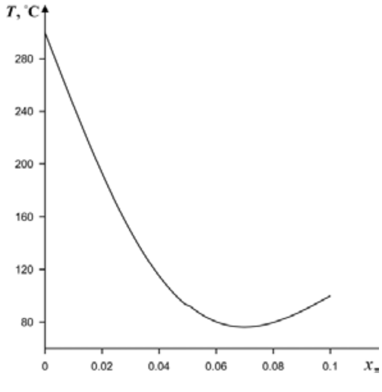

Fig. 4. Temperature distribution over the thickness of the plate at time t = 60 s

The method of computation being examined is obscure, in order to deduce the field of temperature, solving a set of linear equations is necessary. There is also the possibility of utilizing lucid diagrams. Adopting a lucid diagram eliminates the necessity of solving a set of equations. The structure of the stability criterion can be expressed as follows:

$$\frac{T}{h^2} \leq \frac{1}{2} \tag{11}$$

Despite the simplicity of the condition (21), it has a very important drawback: the step is small, and in order to find the temperature value over a large period of time, it is necessary to carry out calculations with many calculations., which in turn leads to the "accumulation" of the calculation error. So, for example, if you take a step of 0.1 in an interval along coordinate x (0,1) and you want to find the temperature value at time 100s, then $M = \frac{100}{2h^2} \approx 2 \cdot 10^5$. Since the above approximation error is of order $O(\tau + h^2)$ to rounding errors can accumulate with such a large number of repetitions of calculations in a clear scheme [7].

CONCLUSION

The issue of distributing temperature in a consistent nucleus with initial-edge conditions is examined. A numerical resolution is available with a finite variation technique and an implicit approximation system. It is demonstrated that computational balance can be attained with a substantial amount of rounds through a discrete plan.

REFERENCES

1 Andrea Bonito, Ricardo Nochetto Geometric Partial Differential Equations. North-Holland, Serial edition, 2020, pp. 50-51.

2 Serge Dos Santos, Mostafa Maslouhi, Kasso A. Okoudjou. Recent Advances in Mathematics and Technology. Proceedings of the First International Conference on Technology, Engineering, and Mathematics, Kenitra, (Applied and Numerical Harmonic Analysis). Morocco, 2020, pp. 26-27.

3 Harald van Brummelen, Alessandro Corsini, Simona Perotto, Gianluigi Rozza Numerical Methods. Flows FEF 2017 Selected Contributions, USA, 2020, pp. 424-425.

4 Inaam Rikan Hassan, Hasan Shakir Majdi, Laith Jaafer Habeeb Fundamentals of Numerical Analysis Techniques for Engineering Applications. India, Scholar Press, 2021. 132 p.

5 Oleg P. Iliev, Svetozar D. Margenov, Peter D Minev, Panayot S. Vassilevski. Numerical Solution of Partial Differential Equations: Theory, Algorithms, and Their Applications. In Honor of Professor Raytcho Lazarov's 40 Years of ... Proceedings in Mathematics & Statistics. Moscow, 2013, pp. 45-46.

6 James Fern, Alexander Rohe, Kenichi Soga, Eduardo Alonso. The Material Point Method for Geotechnical Engineering. A Practical Guide. Holland, CRC Press, 2019. 442 p.

7 Forsythe J., Malcolm M., Mouler K. Mashinnyye metody matematicheskikh vychisleniy. Perevod s angliyskogo Kh.D. Ikramova [Machine methods of mathematical calculations. Translation from English by Kh. D. Ikramov]. Moscow, Mir, 2022. 279 p.

IRSTI 666.9:691.5

PROCESSING OF WASTES FROM CHRYSOTILE ASBESTOS PRODUCTION INTO INDUSTRIAL MAGNESIUM COMPOUNDS

Auyeshov A.P., Auyelbekova Zh.Ye.*, Tasboltayeva A.M.
M. Auezov South Kazakhstan University, Shymkent
***Corresponding author's email:** auelbekova.90@mail.ru

ABSTRACT

This researchproposesnew schemes for magnesium extraction from serpentinite chrysotile-asbestos waste using the acid method. The technology involves using solutions of low concentration of sulfuric acid to extract up to 50% of magnesium from its total content in the composition of the waste in the form of magnesium salts.

The acid-insoluble residue, where the rest 50% of magnesium remains is used to produce silicon-magnesium-phosphorus-containing fertilizers. The use of low-concentration acid solutions makes it possible to obtain magnesium salts of sufficiently high quality, with an impurity content of no more than 1.0%, without special technological complications and difficulties. It is noted that at this time the maximum relevant intended use of mineral acid is achieved. The crystallohydrates of magnesium chloride, magnesium sulfate and magnesium nitrate were obtained, satisfying the requirements of GOST-s quality.

Keywords: serpentinite wastes, chrysotile-asbestos, sulfuric acid method, magnesium sulfate, magnesium chloride, magnesium nitrate.

INTRODUCTION

The consumption of magnesium-containing compounds is an integral part of modern chemical production. Currently, Kazakhstan does not have its own production of industrially important magnesium compounds and magnesium-containing fertilizers. Domestic demand is met by imports.

Having its own magnesium-containing source of raw materials (technogenic raw materials in the amount of 500-600 tons containing 40-45 wt. % of MgO, Zhitikarinskoye deposit of Kostanay region), as well as sulfuric acid production facilities, the most expedient direction to meet the needs of various industries of the Republic of Kazakhstan in magnesium-containing reagents (oxide, hydroxide, nitrate, chloride and magnesium sulfate), as well as magnesium-containing fertilizers, is the organization of their production in the country.

Despite the multiplicity and diversity of the conducted research, there are currently no industrially developed technologies for the disposal of asbestos production waste with the production of magnesium compounds [1].

MATERIALS AND METHODS

In this work, the waste from the production and enrichment of chrysotile asbestos was studied as an object of research from the Zhitikarinsky deposit of JSC "Kostanay minerals", Zhitikara city. Pulverized asbestos-containing wastes are formed mainly as a result of the implementation of technological processes of ore crushing and dust trapping by aspiration systems.

Reagents and acids used for chemical dissolution and analysis of wastes of grades "R2" and "AnalaR" comply with the requirements of GOST 3118-77, GOST 4461-77, GOST 4204-77. All solutions were prepared using distilled water, and a “blue band” filter was used for filtration.

The degree of waste decomposition by acids was controlled and calculated from the yield of magnesium cations into the solution as regard to the thermal potential, based on its content in the waste. The solid precipitate was analyzed using a REM instrument (JSM-6490 LV, JOEL, Japan), complete with JNGA Energy 350 energy dispersive microanalyzer systems.Magnesium was determined according to the standard procedure [2], the content of free acid (H^+) - by tapping with 0,1M NaOH solution [3].

RESULTS AND DISCUSSION

Waste processing according to our developed scheme makes it possible to obtain the following magnesium-containing competitive compounds from serpentinite wastes of chrysotile-asbestos: sulphate, chloride, magnesium nitrate, which meet the requirements of GOSTs in terms of quality, as well as silicon and phosphorus-containing magnesium fertilizers. Thus, magnesium salts - $MgCl_2$, $MgSO_4$, $Mg(NO_3)_2$ are the starting materials for the production of commercial compounds - magnesium oxide, magnesium hydroxide and magnesium metal.

We have determined that 50% of Mg in technogenic waste is located in the brucite layer of the serpentinite structure, and 50% of Mg is located in the inner layer (tube cavity) of molecules. Magnesium from the brucite layer, i.e., 50% Mg of its total content in serpentinite is easily extracted by acids of low concentration, the remaining amount, i.e., 50% Mg (located in the inner layer) can be attributed to the hard-to-recover part of magnesium from the molecular structure of serpentinite during their acid treatment [4].

It has been established that the limiting stage of technological processing is associated with the formation of a hard-to-filter gel form of silica precisely during the extraction of magnesium compound from the inner layer of serpentinite. Depending on the location of magnesium in the structure of serpentinite can be conditionally divided into: easily extractable (located in the brucite layer, 50%) and hardly extractable (located in the inner layer, 50%).

Thus, the developed innovative acidic method of processing serpentinite chrysotile-asbestos waste (CAW) suggests using the easily recoverable part of magnesium (up to 50%) to obtain magnesium salts of sufficiently high quality (with an impurity content of no more than 0.5%), without special technological complications and difficulties with minimal costs. The hard-to-recover part of magnesium (50%), which remains in the composition of the solid residue, after separation (filtration) of the solution of magnesium salts, is used to obtain silicon-magnesium-phosphorus-containing (CMP) fertilizer [5, 7].

The integrated waste processing scheme is shown in Fig. 1.

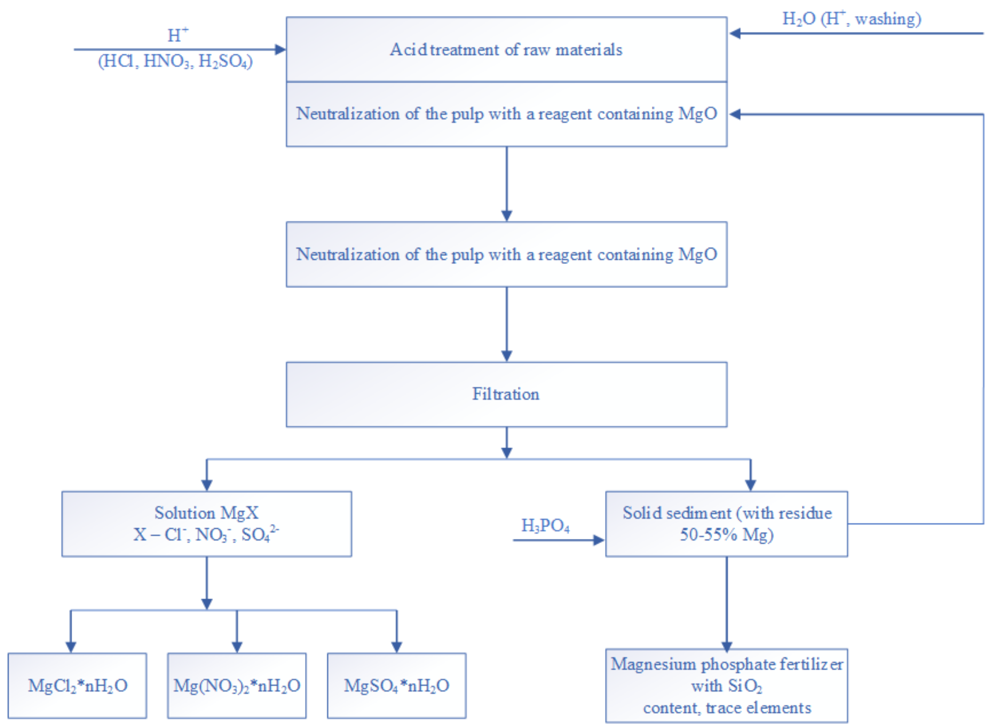

Fig. 1. Basic technological scheme of the complex processing of serpentinite

The study of the effectiveness of using certain types of mineral acids (HCl, HNO_3 and H_2SO_4) as the main reagent (the main consumable of production) for the re-processing of waste indicates the effectiveness of the use of sulfuric acid [6].

When using *sulfuric acid (H_2SO_4)* to obtain magnesium sulphate salt – $MgSO_4$ (at least 99.0%of purity). The resulting $MgSO_4$ can be used to produce magnesium hydroxide $Mg(OH)_2$ and magnesium oxide (MgO) in a "wet" way. The effectiveness of this method is shown in Table 1.

Table 1 - At using sulfuric acid (H_2SO_4) for leaching

Reagents				Products			
Name of consumables	Weight, ton	Price per 1 ton	Amount, USA dollar	Name of processing product	Weight, ton	Price per 1 ton	Amount, USA dollar
Sulfuric acid (H_2SO_4) – 92,5%	1.08 (1 t)	95$	103.78	Magnesim Oxide (MgO)	0.41	4000$	1640
Sodium hydroxide (NaOH) – 99%	0.82 (1 t)	763$	634.36	Sodium Sulfate (Na_2SO_4)	1.44	2003$	2884.69
Total 7			738.14				4524.69

The technological cycle ends with the treatment of the solid residue with phosphoric acid to obtain magnesium-phosphate fertilizers.

Thus, the developed technological scheme makes it possible to comprehensively and cost-effectively process serpentinite waste from the production of chrysotile asbestos.

CONCLUSION

Thus, the developed technological scheme makes it possible to comprehensively and cost-effectively process serpentinite waste from the production of chrysotile asbestos to obtain magnesium salts of sufficiently high quality, with an impurity content of no more than 1.0%, without special technological complications with a high degree of intended acid use.

REFERENCES

1 A.K. Dikanbayeva, A.P. Auyeshov, M.S. Satayev, I.V. Pirminova, Ch.Z. Yeskibayeva and K.T. Arynov. Influence of structural and molecular features of chrysotile on interaction within acid-chrysotile system // Rasayan J. Chem. – Vol. 15. NO. 2, 2022. – P. 979-983.

2 Methods of analysis of brines and salts/Eds. Yu.M. Morachevsky, E.M. Petrova - M.: Chemistry, 1964. – 406p.

3 Analytical chemistry. Chemical methods of analysis/Eds. O.M. Petrukhina. - M.: Chemistry, 1993. – 400p.

4 Mehta P.K. Pozzolanic and Cementitious Byproducts as Mineral Admixtures for Concrete – A Critical Review // Proc. International Conference on the Use of Fly Ash, Slags and Silica Fume in Concrete. – Montebello, Canada ACI/SP – 79 (1983).

5 Arynov K.T., Auyeshov A.P., Yeskibayeva Sh.Z., Darzhanova F.P., Ramyar K. Serpentinite Wastes and Phosphoric Acid Interaction Products Research // «International Conference of Industrial Technologies and Engineering – 2016». – Shymkent, October 28-29, 2016. – P. 188-192.

6 Auyeshov A.P., Arynov K.T., Yeskibayeva Ch.Z., Beisbekova R.D., Alzhanov K.B. Study of Chemical Additives Effect of α- and β-Polymethylenenaphthalenesulfonate upon Properties of Cement Grout and Concrete // Modern Applied Science (Canada, IF=0,224, в печати).

7 Auyeshev A., Verner V., Arynov K., Yeskibayeva Ch., Darzhanova F. Change of the Basicity Coefficient of the Wollastonite Phase in the Process of Charge Thermal Treatment // Industrial technology and engineering. – 2016. – №2(19). – P. 24-30.

IRSTI 669.15-198

THE POSSIBILITY OF JOINT PROCESSING OF KARATAU AND CHILISAY PHOSPHORITES WITH THE PRODUCTION OF FERROALLOYS, CALCIUM CARBIDE AND THE DISTILLATION OF PHOSPHORUS INTO THE GAS PHASE

Karataeva G.E.[1]*, Shevko V.M.[1], Uteyeva R.A.[1], Badikova A.D.[1], Lavrov B.A.[2]
[1]M.Auezov South Kazakhstan University, Shymkent, Kazakhstan
[2]St. Petersburg State Technological Institute (Technical University), Russia, St. Petersburg
***Corresponding author's e-mail**: karataevage@mail.ru

ABSTRACT

The article presents the results of studies of electrothermal production of ferroalloy from a mixture of Karatau and Chilisay phosphorites in the presence of carbon and iron. The studies were carried out using the HSC-6.0 Chemistry software package of the Finnish metallurgical company Outokumpu, based on the Gibbs energy minimization principle. The influence of the amount of carbon and iron on the degree of extraction of silicon into the alloy (the content of silicon in it), calcium into calcium carbide, and phosphorus into the gas phase is determined. It was found that in the system with an increase in the amount of iron from 13 to 39%, the maximum transition of silicon into the alloy up to 77.6% is observed. In the temperature range of 1580-2200^{0}C the formation of FeSi25 grade ferrosilicon from a mixture of phosphates in the presence of 26-39% Fe and 34% C, is observed, and at 2005-2200^{0}C, FeSi45 grade ferrosilicon is formed in the presence of 13-18% Fe and 34% C. At 2000^{0}C calcium carbide with a low volume of 230 dm^3/kg is formed from a mixture of phosphorites in the presence of 48% C and 13% Fe The resulting gaseous phosphorus at a temperature of ≥1000^{0}C regardless of the iron content, is completely extracted into the gas phase in the form of P_2 at a temperature of more than 1500^{0}C.

Keywords: processing, phosphorites, thermodynamic modeling, carbon thermal reduction, iron, ferroalloy, phosphorus, calcium carbide.

INTRODUCTION

The main method of processing Karatau phosphorites is their electric melting to produce gaseous phosphorus. Despite the fact that up to 89.5% of phosphorus is extracted into gas during electric melting, this process is characterized by significant formation of dump slag (at least 10t per 1t of phosphorus) [1]. Processing of phosphorites of the Aktobe deposit containing 10-12% P_2O_5 [2] by electric melting is not economically feasible. Therefore, this is a deposit that contains 500 million tons of P_2O_5 [3] now it is a backup. To improve the integrated use of phosphorites, we have proposed a slag-free technology for their processing to obtain calcium carbide, siliceous ferroalloy with phosphorus distillation [4.5]. This method allows processing substandard phosphate raw materials.

The aim of the work was to thermodynamically simulate the production of a ferroalloy, calcium carbide from a mixture of Karatau and Chilisay phosphorites (a mixture of Karatau and Chilisay phosphorites) in the presence of carbon and iron and phosphorus distillation into the gas phase.

MATERIALS AND METHODS

The research was carried out by the method of thermodynamic computer modeling using the HSC-6.0 software package by the Finnish metallurgical company "Outokumpu" [6], based on the fundamental principle of Gibbs energy minimization. The determination of the equilibrium degree of the distribution of elements by interaction products was considered according to the algorithm [7] developed at M. Auezov SKU.

A mixture of Karatau (50 kg) and Chilisay phosphorites (100 kg) with a ratio of 1:2 was used in the work, which contained, by weight%: 33 $Ca_3(PO_4)_2$, 47.1% SiO_2, 6.8 CaO, 1.9 Al_2O_3, 3.1 Fe_2O_3, 2.2 CaF_2, 1.5MgO, 2.7 $CaSO_4$, 0.3 Na_2O, 0.1 TiO_2, 0.1 MnO, 1.2 $CaCO_3$.

RESULTS AND DISCUSSION

Fig. 1 shows the effect of temperature on the equilibrium quantitative distribution of silicon, calcium and phosphorus-containing substances in the system of a mixture of Karatau and Chilisay phosphorites - C - Fe. The amount of carbon was 51%, and the amount of iron was 13.26 and 39% by weight of the mixture of phosphorites.

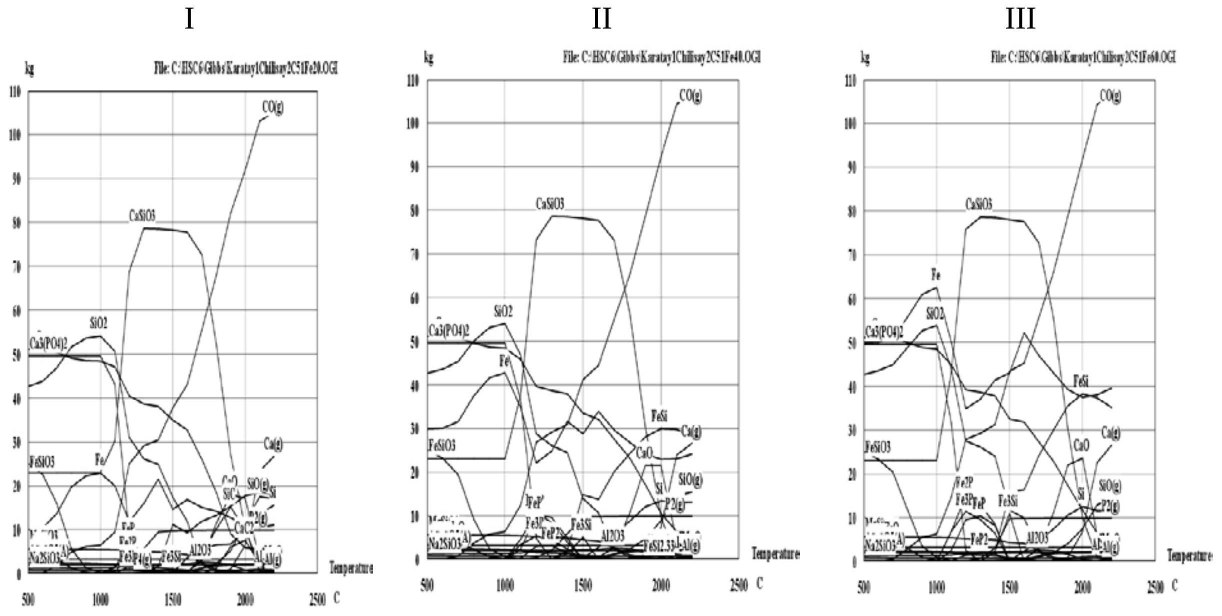

Amount of iron: I – 13%, II -26%, III – 39%

Fig. 1. Effect of Temperature on the Equilibrium Quantitative Distribution of Silicon, Calcium, and Phosphorus-Containing Substances in the System of a Mixture of Karatau and Chilisay Phosphorites - C - Fe

On Fig. 2,3 shows the effect of temperature and iron on the equilibrium degree of distribution of phosphorus, silicon in the system of a mixture of Karatau and Chilisay phophorites - C - Fe. It can be seen that in the temperature range of 1100-1400 ^{0}C some part of phosphorus passes into iron phosphides in the form of Fe_2P, FeP, FeP_2, Fe_3P. The maximum degree of phosphorus conversion to iron phosphides is observed at 1300^{0}C in the presence of 39% iron, amounting to 28.24% for Fe_2P, 37.48% for FeP, 11.16% for FeP_2, 15.07% for Fe_3P. The beginning of the formation of gaseous phosphorus is observed at a temperature of more than 1000^0C. In all systems, regardless of the iron content, gaseous phosphorus is completely extracted into the gas phase in the form of P_2 at a temperature of ≥1500 ^{0}C.

At 500^0C $CaSiO_3$, $FeSiO_3$, $MgSiO_3$, Al_2SiO_5, Na_2SiO_3 are formed in the system. The beginning of silicon extraction of FeSi, Si и Fe_3Si occurs at 1400^0C, $FeSi_2$ - at 1600^0C and SiC, $FeSi_{2,33}$ - at 1700^0C. Moreover, the formation of these substances occurs initially from SiO_2, and then from silicates of calcium, iron, magnesium, aluminum and sodium. The maximum transition of silicon to iron silicides and elemental silicon is observed in the system at 39% Fe and a temperature of 2000^0C. Thus, 38.67% passes into FeSi and 38.02% of silicon passes into the elemental state. The maximum degree of silicon transition to $SiO_{(g)}$ (27.6%) is observed at 2200^0C.

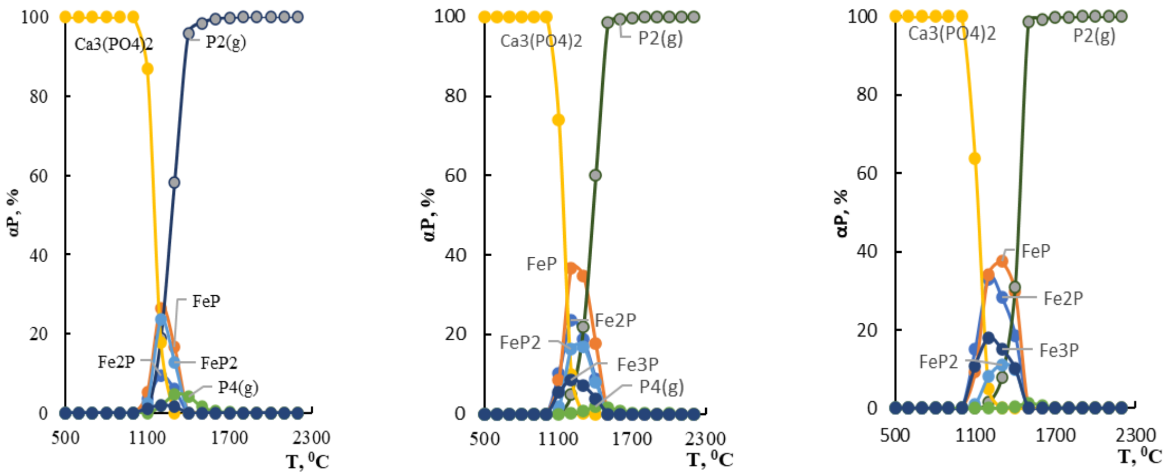

Amount of iron: I – 13%, II -26%, III – 39%

Fig. 2. Influence of temperature and iron on the equilibrium degree of phosphorus distribution

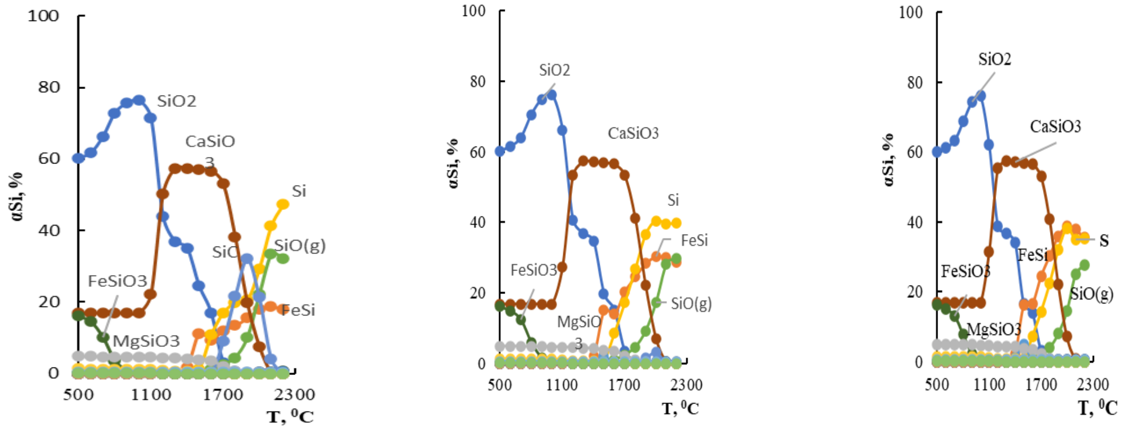

Amount of iron: I – 13%, II -26%, III – 39%

Fig. 3. Influence of temperature and iron on the equilibrium degree of silicon distribution

Table 1 shows that calcium at 500^0C is found in $Ca_3(PO_4)_2$, $CaSiO_3$, CaF_2, CaS. The formation of calcium carbide occurs in the temperature range1800 – 2100 ^{0}C. The maximum degree of transition of Ca to CaC_2 (15.85%) is observed at 2000^0C in the presence of 13% iron. It should be noted that an increase in iron content negatively affects the formation of CaC_2.

Table 1 - Influence of temperature and iron on the equilibrium degree of calcium distribution in the basic substances, % *

Substance	Fe, %	Temperature, ^{0}C										
		900	1000	1100	1300	1500	1700	1800	1900	2000	2100	2200
$Ca_3(PO_4)_2$	13	63.96	63.96	55.71	0.038	0	0	0	0	0	0	0
$CaSiO_3$	13	26.51	26.51	34.78	90.22	89.76	83.45	60.14	31.22	11.94	0.55	0.02
CaO	13	0	0	0.02	0.24	0.68	6.94	27.34	42.8	40.9	7.58	1.26
CaC_2	13	0	0	0	0	0	0.09	2.7	12.81	15.85	4.78	0
CaF_2	13	5.63	5.63	5.63	5.63	5.63	5.63	5.63	5.63	5.63	5.63	5.63
$Ca_{(g)}$	13	-	-	-	-	-	0.01	0.35	3.6	21.8	77.6	89.3

*) In small amounts, calcium passes into CaO, CaF_2, CaS.

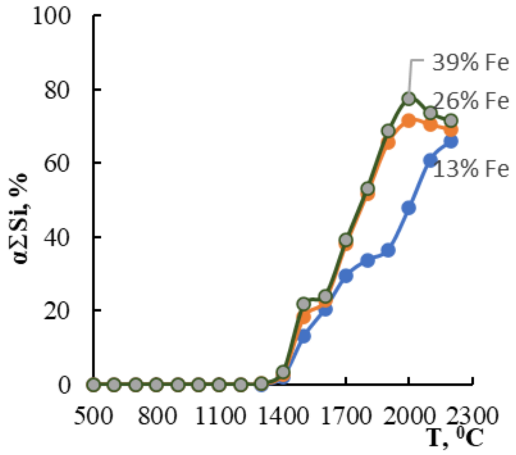

Fig. 4. Influence of temperature and iron on the total degree of transition of silicon to ferroalloy

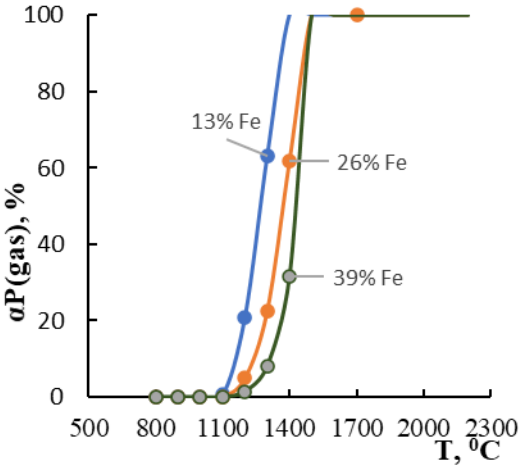

Fig. 5. Influence of temperature and iron on the total degree of phosphorus transition to the gas phase

Fig. 4 provides information on the effect of temperature and the amount of iron on the total degree of transition of silicon into a ferroalloy ($\alpha Si_{(alloy)}$). It can be seen that with an increase in temperature and the amount of iron $\alpha Si_{(alloy)}$ increases, while the maximum αSi(alloy) is 77.7% at a content of 39% iron. Fig. 5 shows the effect of iron on the total degree of transition of phosphorus to the gas phase. It can be seen that in the temperature range from 1100 to 1500^0C an increase in the amount of iron from 13 to 39% makes it possible to increase the extraction of phosphorus into gas. At a high temperature, phosphorus, regardless of the amount of iron, completely turns into gas. The effect of temperature and iron on the silicon concentration in the alloy is shown in Fig. 6. To determine the optimal parameters, we combined the results of the silicon concentration in the alloy. The concentration of silicon in the alloy increases with increasing temperature to a maximum of 47.52% at 2200^{0}C and 13% iron. It can be seen from Figure 6 that in the formation system of FeSi25 grade ferrosilicon occurs in the *abdfn* region, and FeSi45 grade ferrosilicon in the *zyx* region. Table 2 shows the values of technological parameters at the boundary points of the *abdfn* and *zyx* regions.

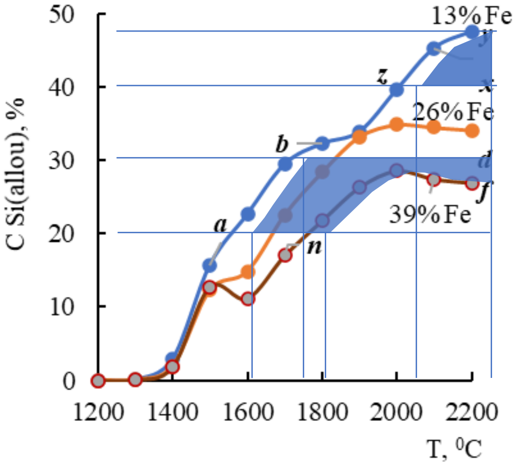

Fig. 6. Influence of temperature and iron on the silicon concentration in the alloy

Table 2 – Technological parameters at the boundary points of Figure 6

Point in Figure	Technological parameters					Ferrosilicon brand
	T, ^{0}C	Fe, %	C Si$_{(alloy)}$, %	αSi$_{(alloy)}$	L, dm^3/kg	
a	1580	26.0	20.0	20.4	0.0	FeSi25
b	1700	26.0	30.0	38.1	0.0	
d	2200	33.6	30.0	70.4	0.9	
f	2200	39.0	27.0	71.5	0.0	
n	1770	39.0	20.0	50.6	0.0	
z	2005	13.0	41.0	48.3	60.3	FeSi45
y	2200	13.0	41.0	66.0	0.0	
x	2200	18.0	47.5	57.3	34.6	

Table 2 shows that during the formation of FeSi25 ferrosilicon, calcium carbide is formed. It is formed in the case of the formation of FeSi45 ferrosilicon [8].

CONCLUSION

Thermodynamic studies of the joint processing of a mixture of Karatau and Chilisay phosphorites have shown that:

- the resulting calcium carbide has a low litre. To increase it, studies were carried out with an increase in the amount of carbon in the system at 20% Fe and 2000 ^{0}C from 34 to

48% of the mass of the mixture. The litre of calcium carbide (dm^3/kg) increases as follows: 62.9 (34%C); 138 (40%C); 186 (44%C) and 230 (48%C). At the same time, the degree of silicon extraction into the alloy decreases to 50.8%.

- an increase in the amount of iron from 13 to 39% makes it possible to convert silicon into an alloy up to 77.6%.
- calcium carbide with a maximum litre of 230 dm^3/kg is formed from a mixture at 2000^0C, 48%C and 13% Fe.
- FeSi25 grade ferrosilicon is formed from a mixture of phosphates in the presence of 26-39% Fe, 34% C in the temperature range 1580-2200^0C, and FeSi45 grade in the presence of 13-18% Fe, 34% C in the temperature range 2005-2200^0C.

REFERENCES

1 Kozlov K.B., Lavrov B.A. Poluchenie karbida kal`ciya v dugovoj pechi i ego analiz. Metodicheskie ukazaniya k laboratornoj rabote. – St. Petersburg. SPbGTI (TU), 2011. 24 p. *«Obtaining calcium carbide in an arc furnace and its analysis»*

2 Ershov V.A., Pimenov S.D. E`lektrotermiya fosfora. Leningrad. Ximiya. 1996. 248p. *«Phosphorus electrothermia»*

3 Evenchik S.D., Brodskij A.A. Texnologiya fosforny`x i kompleksny`x udobrenij. – Moscow.: Ximiya, 1987. 464 p. *«Technology of phosphorous and complex fertilizers»*

4 Shevko V.M., Uteyeva R.A., Badikova A.D., Lavrov B.A. *Sposob pererabotki fosforita*. Patent RK, no. 35033, 2021.

5 Shevko V.M., Badikova A.D., Uteeva R.A. Komp`yuternoe termodinamicheskoe modelirovanie vliyaniya temperatury` i davlenie na vzaimodejstvie v sisteme $Ca_3(PO_4)_2$-C-Fe-SiO_2// Sbornik nauchny`x statej XXVI MNPK «Innovaciya-2022» (Tashkent, 26-27 oktyabrya). – Tashkent, 2022. P.52-55. *«Computer thermodynamic modeling of the effect of temperature and pressure on the interaction in the* $Ca_3(PO_4)_2$-C-Fe-SiO_2 *system»*

6 Udalov Yu.P. Primenenie programmny`x kompleksov vy`chislitel`noj i geometricheskoj termodinamiki v proektirovanii texnologicheskix processov neorganicheskix veshhestv. St. Petersburg. SPbGTI (TU), 2012. 187 p. «*Application of software complexes of computational and geometric thermodynamics in the design of technological processes of inorganic substances»*

7 Shevko V.M., Serzhanov G.M., Karataeva G.E., Amanov D.D. Raschet ravnovesnogo raspredeleniya e`lementov primenitel`no k programmnomu kompleksu HSC-5.1. Svidetel`stvo o vnesenii svedenij v gosudarstvenny`j reestr prav na ob``ekty`, oxranyaemy`e avtorskim pravom. Programma dlya E`VM, RK №1501 ot 29 yanvarya 2019. *«Calculation of the equilibrium distribution of elements in relation to the HSC-5.1 software package»*

7. GOST 1415-93 (ISO 5445-80). Mezhgosudarstvenny`j standart. Ferrosilicij. Texnicheskie trebovaniya i usloviya postavki. Mezhgosudarstvenny`j sovet po standartizacii, metrologii i sertifikacii. - Minsk, 1993. 11p. (izmeneniya №1, protokol №26 ot 8 dekabrya 2004). *«Interstate standard. Ferrosilicon. Technical requirements and delivery conditions»*

IRSTI 66.047

STUDY OF THE TECHNOLOGICAL EQUIPMENT OF THE DRYING DRUM UNIT FOR AIR CLEANING FROM DUST

Abdoluly K.[1], Mussabekov A.A.[1*], Dzhanaliyev B.M.[1], Yeshmaganbetova S.[2], Altynbekov R.F.[1]

[1]M. Auezov South Kazakhstan University, Shymkent, Kazakhstan
[2]Miras University, Shymkent, Kazakhstan
[*]**Corresponding Author's email:** musabekov_a@rambler.ru

ABSTRACT

The article discusses three stages of the dedusting process and the use of various methods and devices for removing aerosol impurities from the air. The process of dusting various objects in most cases consists of steps such as dust removal prevention, dust collection and dust distribution. The results of studies to determine the functional dependence of the filling coefficient on the operating parameters of the drum drying unit are shown. As a result of the analysis and generalization of the data obtained, it was found that the coefficient of filling the drum with material and the time of residence of the particles in the apparatus depend on the angle of the drum, the speed of its rotation. It is shown how to solve the problem of improving the efficiency of the drying unit by combining high wet material and basic drying pretreatment.

Keywords: technological modernization, dedusting process, trapping, filling factor, regime parameters.

The need for "technological modernization of the Kazakhstani economy" covers economic efficiency, product competitiveness and, above all, technological improvement. A large amount of industrial wastes and emissions that are released during technological processes have the greatest harm, first of all, for residents of populated cities and nearby villages.

Thereby, in the future, it will be necessary to attract new innovative technologies, modern devices and units that give minimal emissions, in which nature itself will contribute to the necessary extent to reduce environmental damage.

Basically, technological processes are aimed at obtaining various dusty materials from small particles. These are cement, building gypsum, flour, etc. These small particles, which are carried by wind currents, form an aerosol stream, the main characteristic of which is the dispersion of dust (particle size) and density, on which the efficiency of its deposition in gravitational and inertial dust collectors depends, respectively, the adhesion of dust particles, which is determined by its adhesive properties.

The whole process of dedusting various substances always consists of three stages [1, 2]: dust prevention (DP), dust collection (DC) and dust dispersion (DD). A certain stage can be carried out by various methods (aerodynamic, hydrodynamic, electromagnetic, thermophysical, mechanical, etc.), which are determined by the nature of directed external influences on dust aerosol.

Dust dispersion (DD), which is present after the previous stages, is to increase the dispersion of dust particles in the atmosphere.

In general, the air purification system from dust may contain several types of equipment, which are connected in a series circuit in order to increase the efficiency of dust collection. Currently, various methods and apparatus are used to capture aerosol impurities from the atmosphere. In production and industry, in such cases, gravitational units are often used, inertial dry and wet, filtering in a porous layer and in an electric field. The main types of inertial dry dust collectors include louvers, cyclones and multicyclones, for wet dust collectors – hollow and packed, foam, shock-inertial action scrubbers, as well as Venturi scrubbers.

When choosing equipment when forming a dust collection system, it is always necessary to take into account the specific requirements of production, the physical-mechanical and physicochemical properties of dispersed particles.

The simplest methods of recycling wastes from current production processes do not provide the proper degree of purification so as not to damage the environment. For example, simple dust collectors – settling chambers, louvres, cyclones – can be used continuously in a two-stage cleaning scheme for pretreatment of wastes. When choosing dust collecting equipment, it is necessary to pay attention to the main characteristic of the unit – the cleaning efficiency.

To capture dust, consider a drum drying unit (Fig. 1), consisting of a base 1, a screw 2, to adjust the angle of the drum, a movable frame 4, fixed to the base 1 by means of a hinge 3.

A drum 11, which is a metal cylinder with a diameter D_d=0.516 m and a length L_d = 1.6 m is fixed on the frame 4 on support rollers 7.

The rotation of the drum 11 is carried out by an asynchronous electric motor 5 through a worm gear 6 by means of a chain transmission 19. Loading and unloading hoppers 8, 9 are installed on the movable frame 4. A fan 16 and a heater 17 are installed to supply and prepare the drying agent, which, after passing through the drying drum, is thrown into atmosphere through a cyclone 18. The material is supplied by a screw feeder 12 through a chute 15. In order to smoothly change the performance of the feeder, a DC electric motor 13 and a worm gear 14 are used to drive it.

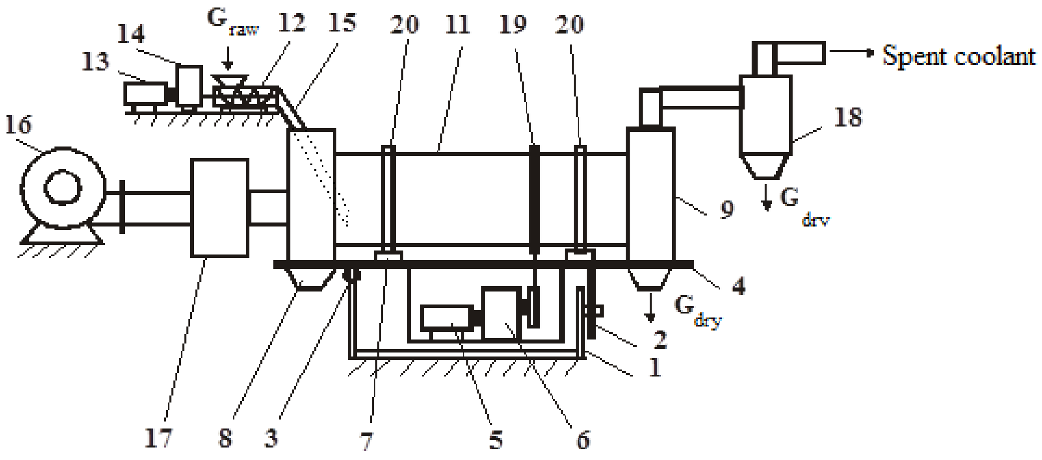

Figure 1 – Dry drying unit scheme

Fig. 1. Drum drying unit scheme

It is known that the residence time of material particles in the drum is functionally dependent on the amount of material present in the drum at a time, i.e., from the filling coefficient ψ. Thereby, studies were also carried out to identify the functional dependence of the coefficient ψ on the operating parameters of the drying drum unit.

It was revealed that the function of the filling coefficient $\psi=f(n)$ has the opposite trend at positive and negative slope angles (Fig. 2 and 3). It can be seen that in the case of installing the drum with a slope towards the loading of the material (Fig. 2), with an increase in the drum rotation speed n, the filling coefficient increases. Under the same conditions, but with the drum inclined towards unloading (Fig. 3), an inverse relationship is observed. Moreover, the values of the filling coefficient themselves differ. So, with a negative α, the coefficient ψ has higher values than with a positive slope angle [2].

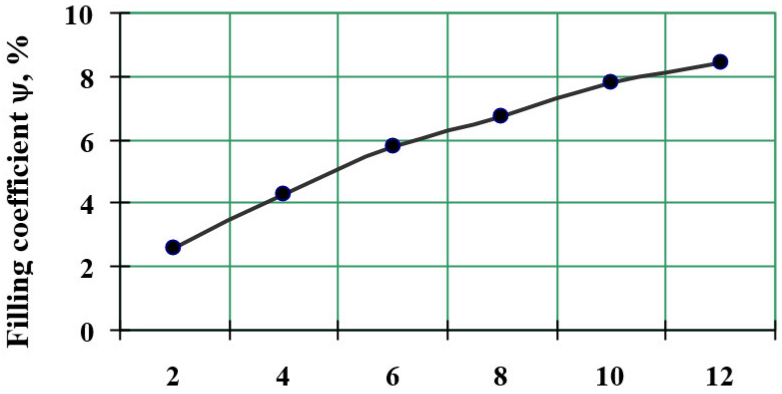

At $\alpha=-1^0$; n=4.16 rpm; ρ_m=560kg/m^3.

Fig. 2. Dependence of the drum material filling coefficient on the drum rotation speed

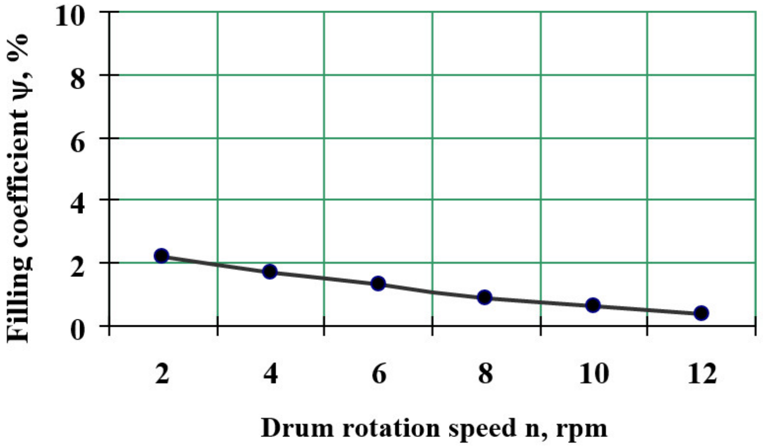

At $\alpha=1^0$; n=4.16 rpm; ρ_m=560 kg/m^3.

Fig. 3. Dependence of the drum material filling coefficient on the drum rotation speed

After the unit enters the stationary mode of operation, it stops and all the material in the drum is unloaded from it, weighed, and the filling coefficient of the unit is calculated according to the following dependence [2]:

$$\psi = \frac{100\, G_{res}}{V_d \;\; \rho_{bulk}}, \tag{1}$$

where G_{res} – the material mass in the drum, kg;
V_d – the drum volume, m^3;
ρ_{bulk} – the bulk density of the material, kg/m^3.

In the study, two types of blades were used: fixed L-shaped and self-shaking. As a result of the analysis and generalization of the obtained data, it was revealed that the coefficient of filling the drum with the material and the residence time of the particles in the apparatus depend on the drum angle, its rotation speed, the coolant speed in the drum, and the nozzle efficiency coefficient. It was established that the average residence time of the dried material in the apparatus with a roller belt drying unit can be calculated with an accuracy sufficient for engineering calculations using the well-known equation:

$$\tau = (1 - k_{fill})\frac{G_a}{G}, \tag{2}$$

where G_a – the weight of the material in the drum at one time, kg;
G – the apparatus efficiency, kg/s;
K_{fill} – the filling coefficient.

The material weight G_a is calculated by the formula [3, 4]:

$$G_a = \frac{\pi D_d^{\;2}}{4} L_d \, \psi \;\; \rho_{,} , \tag{3}$$

where $D_б$ – the drum diameter, m;
L_d – the drum length, m;
ρ_{bulk} – the bulk density of the material, kg/m^3.

When developing the design of the drying unit, the problem of increasing its efficiency is solved by combining two zones (pretreatment of high-moisture material in a boiling bed 1 and main drying II) with simultaneous intensive mixing, uniform distribution over the cross section of the drum and separation of particles depending on their size. This task is implemented in an apparatus containing a stationary drum with cylindrical holes for supplying gas to the boiling bed 1 and conical holes with a diameter equal to 50% and 75% of the average equivalent particle diameter (d_e) for their separation according to the fractional composition, drilled along the arc of the drum with an angle of 60°, fitting pipes for the inlet and outlet of the coolant and the solid phase, a rotating shaft with peripheral charge blades fixed on it by means of spokes, gaskets to prevent gas leakage in a shaft – wall coupling, the shaft support devices and a drive station, hoppers for unloading the dried material.

Analyzing the proposed technical solution with a similar design, it can be concluded that the proposed device differs from the known one by combining drying processes of two classes – in a boiling bed and in a semi-suspended state [5-7], the presence of an L-shaped blade peripheral nozzle movable relative to the drum, and also the presence of separation holes for separating fine particles as they dry, which are cone-shaped with an angle of 60 to prevent them from clogging with particles.

REFERENCES

1 Yunin V.A. Process sushki izmelchennogo rastitelnogo materiala v barabannoj sushilke [The process of drying the crushed plant material in a drum dryer] // Izvestiya NV AUK. 2020. 1(57). P. 335-349. DOI: 10.32786/2071-9485-2020-01-33.

2 Altukhov A.V., Zhukova T.A., Balabekov M.O., Altukhova A.A. Intensifikatsiya barabannykh sushil'nykh apparatov [Intensification of drum dryers]. Trudy Mezhdunarodnoy nauchno-tekhnicheskoy konferentsii «Aktual'nyye problemy sushki i termovlazhnostnoy obrabotki materialov» [Proceedings of International Scientific and Technical Conference «Actual problems of drying and thermal and moisture processing of materials»]. Voronezh, 2010, pp. 534-538.

3 Voblikova, T.V. Processy i apparaty pishhevyx proizvodstv. Uchebnoe posobie / T.V. Voblikova, S.N. Shlykov, A.V. Permyakov. – Stavropol: AGRUS Stavropolskogo gos. agrarnogo un-ta, 2013. – 212 p.

4 Altukhov A.V. Metodologiya sovershenstvovaniya i rascheta barabannykh sushil'nykh agregatov. Avtoreferat dissertatsii doktora tekhnicheskikh nauk [Methodology for improving and calculating drum drying units. Abstract of Dissertation for the degree of Doctor of Technical Sciences]. Shymkent, 1999. 50 p.

5 Serimbetov B.A. Raschet i modelirovaniye barabannykh sushil'nykh apparatov s podvizhnym raspredelitel'nym ustroystvom. Avtoreferat dissertatsii na soiskaniye uchenoy stepeni kandidata tekhnicheskikh nauk [Calculation and modeling of drum drying units with a movable distribution device. Abstract of Dissertation for the degree of Candidate of Technical Sciences]. Shymkent, M. Auezov SKSU, 1999. 27 p.

6 Lykov M.V. Teoriya sushki [Theory of drying]. Moscow, Energiya, 1968. 254 p.

7 Chernobylsky I.I., Tonanaiko Yu.N. Sushil'nyye ustanovki khimicheskoy promyshlennosti [Drying installation of chemical industry]. Kyiv, Tekhnika, 1969. 279 p.

IRSTI 66.098

ANALYSIS OF THE STAGES OF BIOGAS PRODUCTION BASED ON AN ORGANIC RENEWABLE SUBSTRATE

Bitemirov R.K.[1], Mussabekov A.A.[1*], Kocherova A.N.[1], Manatkyzy Zh.[2], Amangeldy T.T.[1]

[1]M. Auezov South Kazakhstan University, Shymkent, Kazakhstan
[2]Miras University, Shymkent, Kazakhstan
[*]**Correspondent Author's Email:** musabekov_a@rambler.ru

ABSTRACT

In the energy sector, there is great interest in the process of producing biogas. This technology for the disposal of food waste based on biogas production technology makes it possible to dispose of organic waste and food waste in biogas plants with minimal losses for the benefit of agriculture and the population. The article discusses the use of biogas technology and the phases of the fermentation process with the help of various groups of bacteria, metabolic products and the division of organic substances into individual components. Thanks to the construction of biogas plants, the widespread introduction of this technology can be relevant for the food industry, gastronomy, large restaurants, catering establishments and agriculture in general. The limits of temperature modes affecting the activity of bacteria and the need for accurate control of the operation of the biogas plant and the assembly of a special automation system are also indicated.

Keywords: biogas, technology, bacteria, temperature regime, substance.

INTRODUCTION

At present, the tendency for biogas production processes is increasing all over the world – this is expressed not only in an increase in the number of planned and built biogas plants, but also in the expansion of a number of farms, housing and communal sector enterprises, various industries and country houses. Consumers are more interested in the problem of decentralization of the energy industry along with the construction of biogas plants. For agriculture, most catering establishments and canteens that have food waste, it is necessary to process this food waste, and it is in this case that biogas processing technology makes it possible to dispose of food waste at a low cost in biogas plants to extract energy and heat. This type of waste and organic conversion is attracting more and more customers from the public and recycling companies, who have recognized its advantages and benefits to the environment. This means that at this time the need for information about this modern technology of biodegradation without air is only increasing.

When organic matter is decomposed by the respective bacteria, biogas is generated. At the same time, in the process of metabolism, a compound of gases is generated, which is called biogas. In this mixture combustible methane (CH_4) is from 5 to 85% and will be the main component of biogas and the main substance for creating and generating power. All power extracted from this combustible methane mixture is considered to be renewable, since the methane is extracted from an organic, renewable substrate. The possibilities of organic substrates, which are taken for the extraction of methane, are very large compared to what is currently used.

When using biogas technology, there are the following stages in the process of extracting biogas from organic matter [1, 2]:

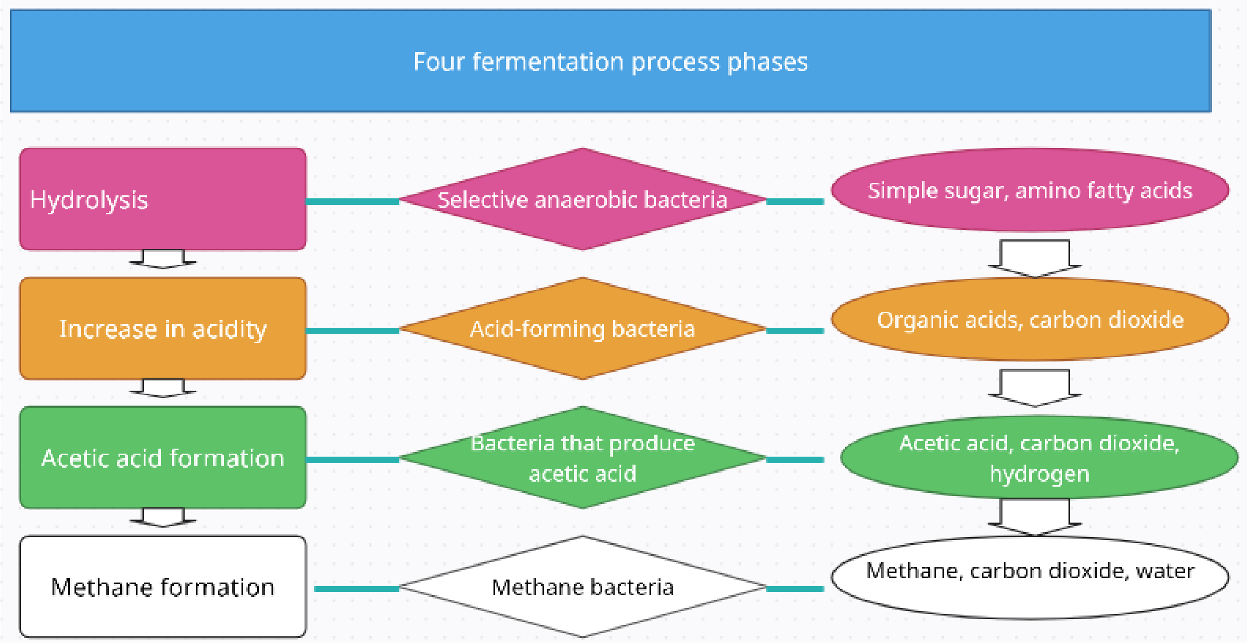

Fig. 1. Biogas extraction process stages

Biogas is a metabolic product that is formed by the action of a bacterium on an organic substrate. During decomposition, 4 stages can be distinguished (Fig. 1), where a number of bacteria take part in various stages:

1. At the 1^{st} stage, aerobic bacteria, with the participation of enzymes, convert high-molecular organic components (protein, carbohydrates, fat, cellulose) into low-molecular components, for example, into sugar, amino acids and water. Enzymes formed by waterlytic bacteria attach to the bacteria from the outside (called an exoenzyme) and then break down the organic components of the substrate into small molecules that can be dissolved in water. Polymeric substances are converted into one-dimensional or separate molecules. This action, called the hydrolysis process, is long lasting and dependent on extracellular enzymes such as cellulose, amylases, proteases and lipases. The pH level (4.5-6) and time constantly influence the process that takes place in the tank.

2. Bacteria that form acids divide the remains of high-molecular organic components into molecules. Some molecules penetrate into bacterial cells, where decomposition continues. Anaerobic bacteria do not always participate in decomposition, consuming the remainder of oxygen and creating an anaerobic environment necessary for methane bacteria. At the pH value of 6.0-7.5, unstable fatty acids, low molecular weight alcohols and gases are first formed (Fig. 2). This stage is called the oxidation stage.

3. Subsequently, bacteria that form acids from organics generate primary substances for the formation of methane. These carbon-reducing bacteria are highly susceptible to temperature changes.

4. In the final phase, methane, carbon dioxide and water are formed as a by-product of methane bacteria containing acids, carbon and hydrogen. During this period, 90% of all methane is formed.

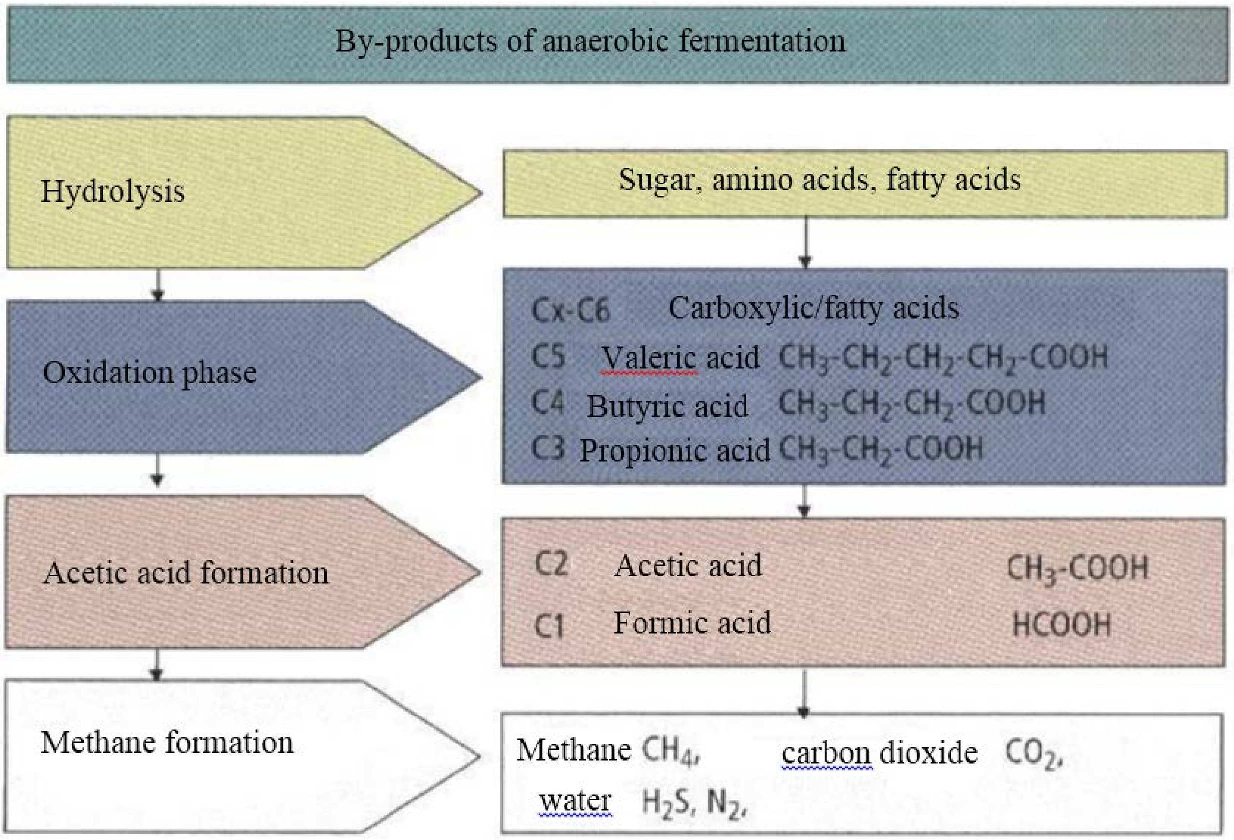

Fig. 2. Fermentation metabolism

Decomposition of organic matter into individual components and transformation into methane occurs only in an environment with moisture, since bacteria can process substances only in a dissolved state [3-5].

MATERIALS AND METHODS

The analysis of the stages of biogas production based on an organic renewable substrate includes the assessment and measurement of various parameters and characteristics of the biogas fermentation process. The main analysis methods used to assess the stages of biogas production are listed below:

Chemical analysis of the substrate: Determination of the content of organic and inorganic components in the substrate, such as the content of solids, organic matter, nitrogen, phosphorus, fat and other nutrients. This helps to determine the nutritional value of the substrate and its potential for biogas production.

Biogas Potential Assessment: Determination of the methane potential (BMP) of the substrate, which indicates its ability to generate biogas. This method is usually based on anaerobic batch testing (APT), during which the volume and composition of biogas produced from a certain volume of substrate over a certain period of time is measured.

Fermentation process monitoring: Measurement of parameters such as pH, temperature, methane concentration, gas pressure level, organic nitrogen content and other relevant parameters during fermentation. This allows you to monitor the process and identify possible problems or violations that may affect the production of biogas.

Gas Chromatography (GC) and mass spectrometry (MS): Used to analyze the composition of biogas, determine the percentage of methane, carbon dioxide (CO2) and other gas components. This helps to determine the efficiency of the process and control the quality of the biogas produced.

Analysis of biological indicators: Determination of the activity and diversity of microorganisms in the biogas system using molecular biology methods such as polymerase chain reaction (PCR), DNA sequencing and fluorescent in situ hybridization (FISG). This makes it possible to study the structure of microbial communities and identify the main groups of microorganisms responsible for the process of biogas fermentation.

RESULT AND DISCUSSION

It was established that in installations that operate on renewable raw materials, higher temperatures occur compared to the laying of additional heating. The anaerobic process is not high temperature, unlike composting; and methane has much more energy. A large amount of easily processed substrate, which is a plant, leads to irreversible oxidation reactions with a corresponding release of heat.

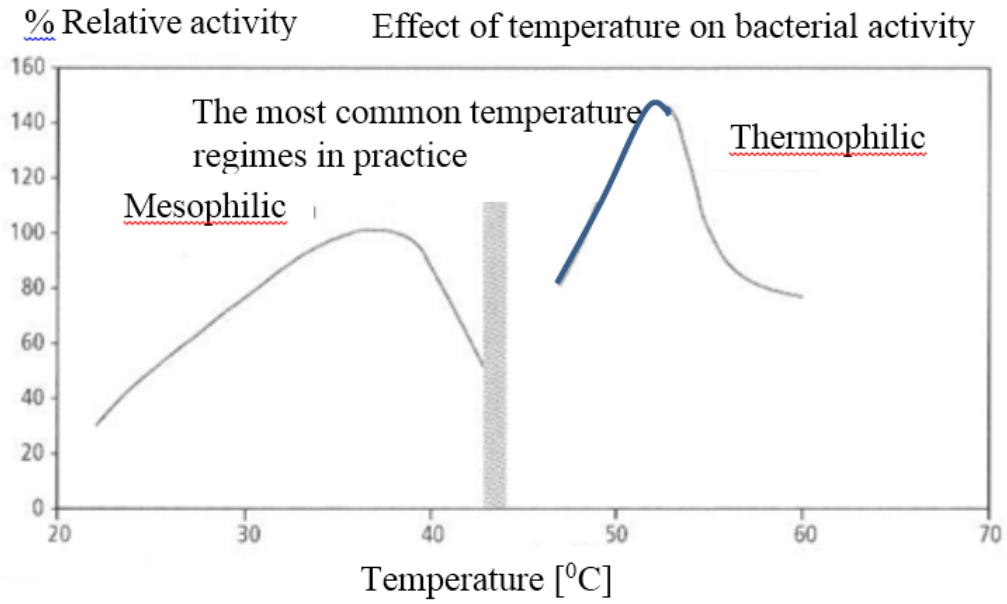

Fig. 3. Effect of temperature on bacterial activity

When working in high temperature conditions (Fig. 3), it is necessary to install special automation systems and precise control of the biogas plant. At present, if biogas plants are fully integrated into agricultural cooperatives, it must be taken into account that they will operate at a high fermenter temperature, so a biogas plant is a special type of production and it is necessary to create an appropriate automation area [3-7].

CONCLUSION

Thus, for a long time (1 month or more), bacteria get used to the new temperature regime, and each agricultural cooperative must choose the best installation option for itself. Various methods of biogas production can also be reduced to several options in terms of process specifications. The fundamental difference between the methods of operation of various plants lies in the method of supply (batch / flow methods), in the form of mixing, in a single-stage or multi-stage system.

REFERENCES

1. Barbara Eder, Heinz Schulz. Biogas plants. Practical guide. Translation from German. Zurich, Zorg Biogas, 2008. 168 p.
2. IEA Bioenergy Task 37 - Country Briefs for 2019. Available at: http://task37.ieabioenergy.com/country-reports.html.
3. Shpilrain E.E. Vozobnovlyayemyye istochniki energii i perspektivy ikh ispol'zovaniya [Renewable energy sources and prospects for their use]. Novoye v rossiyskoy elektroenergetike - New in the Russian Electric Power Industry, 2004, No. 8, pp. 6-15.
4. Curto D, Martín M. Renewable based biogas upgrading. Journal of Cleaner Production [Internet]. 2019 Jul;224:50–9. Available at: http://dx.doi.org/10.1016/j.jclepro.2019.03.176
5. Dębowski M, Zieliński M, Grala A, Dudek M. Algae biomass as an alternative substrate in biogas production technologies—Review. Renewable and Sustainable Energy Reviews [Internet]. 2013 Nov;27:596–604. Available at: http://dx.doi.org/10.1016/j.rser.2013.07.029
6. Briot P, Dehame J, Desaphix A, Nachidi M, Tadeo F. Design and Analysis of a Renewable Hydrogen system for biogas production. 2022 13th International Renewable Energy Congress (IREC) [Internet]. 2022 Dec 13; Available at: http://dx.doi.org/10.1109/irec56325.2022.10002092
7. Casson Moreno V, Papasidero S, Scarponi GE, Guglielmi D, Cozzani V. Analysis of accidents in biogas production and upgrading. Renewable Energy [Internet]. 2016 Oct;96:1127–34. Available at: http://dx.doi.org/10.1016/j.renene.2015.10.017

INDUSTRIAL TECHNOLOGY AND ENGINEERING

Technical editor: *Nazarbek U.*

Signed for print on 24.03.2023

Format 70x100 1/16. Offset paper

Accounting-publishing list

Circulation 300 copies

CONTENTS

ISSN 2223-3911
02
9 772223 391166